University of South Carolina
Scholar Commons

Theses and Dissertations

Summer 2020

Design of High Efficiency Wireless Power Thansfer System With Nonlinear Resonator

Yibing Zhang

Follow this and additional works at: https://scholarcommons.sc.edu/etd

Part of the Electrical and Computer Engineering Commons

Recommended Citation

DESIGN OF HIGH EFFICIENCY WIRELESS POWER THANSFER
SYSTEM WITH NONLINEAR RESONATOR

by

Yibing Zhang

Bachelor of Engineering
Renai College of Tianjin University, 2017

Submitted in Partial Fulfillment of the Requirements

For the Degree of Master of Science in

Electrical Engineering

College of Engineering and Computing

University of South Carolina

2020

Accepted by:

Guoan Wang, Director of Thesis

Xiaofeng Wang, Reader

Cheryl L. Addy, Vice Provost and Dean of the Graduate School

DEDICATION

To my advisor Guoan Wang and my parent

ABSTRACT

Wireless power transfer technology (WPT) has been rapidly developed in recent years. The primary benefit of WPT is that it replaces the traditional wire charging with a cordless charging method. WPT technology has been applied in many fields, such as bio-implants, electric vehicles, and wirelessly charging systems. According to the different energy transmission mechanism, WPT technology can be divided into magnetic field coupling (includes magnetically coupled inductive and magnetically-coupled resonant), microwave radiation, laser emission, electrical-field coupling, and ultrasonic transmission type. Among these technologies, the magnetic resonance coupling method has a better promise because of its long transfer distance and high efficiency. However, there are some questions that need to be resolved, among which the most prominent is that the technology has a low tolerance to the variations of the coupling factor because of the frequency splitting phenomenon, which would lead to transmission efficiency degradation of magnetic resonance coupling WPT systems. Hence, based on reviewing the research status and trend of WPT technology, this paper analyses the frequency splitting phenomenon of the wireless power transfer system, discusses the duffing resonator circuit and its properties, and designs a kind of high-efficiency wireless power transfer inductive system with both non-linear inductors and non-linear capacitors. The main research works of this paper are as follows:

Firstly, aiming at the frequency splitting problem during magnetic coupled resonance wireless power transmission, the frequency splitting phenomenon for the wireless power transfer system is studied by an electric circuit model method. The expression of the relationship between the load voltage, transmission efficiency, and coupling factor was derived, and the law of frequency splitting is discussed. Furtherly, an analysis of frequency splitting based on simulation also presented. Finally, the frequency splitting suppression method is proposed. The above research work provides a theoretical basis for solving the problem of frequency splitting and designing a kind of high-efficiency WPT system.

Subsequently, a duffing resonator circuit with a nonlinear capacitor, which can eliminate the frequency splitting and keep the high transmission efficiency and power delivered to the load is developed. With the help MATLAB software, the properties of the duffing resonance circuit are discussed furtherly. The results show that the duffing resonance circuit has significantly wider bandwidth than the conventional linear resonance circuit while achieving a similar amplitude level.

Finally, the high efficiency non-linear wireless power transfer system based on non-linear inductors with ferromagnetic thin film core and non-linear capacitors with ferroelectric thin film dielectrics is designed. Moreover, the system's performance is improved, the range of coupling factors significantly extended while both load power and high PTE were maintained. The reason for the high efficiency of the system is furtherly discussed, and the research result shows that non-linear inductor with ferromagnetic thin film core has variable inductance which can be synchronously changed along with the current through the inductor in the circuit. The non-linear capacitor with ferroelectric thin

film dielectrics can also have variable capacitance, which can be synchronously changed along with the voltage applied to the capacitor. However, the voltage across the capacitor and current through the inductors are different initially, high power transmission efficiency can be achieved by self-tuning capability of inductance and capacitance from the film based non-linear resonators.

Research results of this paper can lay the solid foundations for the application of WPT technology in the fields of bio-implants, electric vehicles, wirelessly charging systems, etc.

TABLE OF CONTENTS

LIST OF TABLES

LIST OF FIGURES

LIST OF SYMBOLS

P_L Load power

L_1 First coil inductance

L_2 Second coil inductance

N_C Nonlinear capacitor

N_L Nonlinear inductor

V_S Source voltage

U_e Equivalent thevenin voltage

LIST OF ABBREVIATIONS

EV ....Electrical Vehicle

MDR ....Multidrug Resistance

MCI-WPT .... Magnetically-coupled inductive WPT

NC ....Nonlinear Capacitor system

NCNL...Nonlinear Capacitor and Nonlinear Inductor system

PTE .... Power Transfer Efficiency

WPT .... Wireless Power Transfer System

CHAPTER 1

OVERVIEW

1.1 Characteristics and application of wireless power transmission technology

The wireless power transmission technology (WPT) is a new power transmission technology, which achieved power transmission without electrical contact from the power supply to the load by electromagnetic effect or energy exchange function. Comparing with the traditional wire transmission technology, it has advantages of safe and reliable and so on, especially in some applications. Therefore, it has been paid more and more attention [1]-[7]. In recent years, the growth momentum of WPT technology has become more powerful, which has gone from theoretical to commercialization, especially in bio-Implants, electric vehicles, and wirelessly charging systems etc. The two application examples of WPT technology are introduced as follows:

Wireless charging is also widely used in electric vehicle charging [6]. The basic concept of the wireless power transfer system of EV structure is shown in figure 1.1. The RX coil is implanted at the bottom of the electric vehicle. Through the redesigned RX coil structure, which is a circular and bar-shaped core, the total size of this coil is reduced by 30%, and the core loss reduces by 17.5% comparing to the traditional wireless charging. This cordless charging technology could make charging convenient, and the EV can be charged anytime and anywhere, like the technology in [7].

1

When people drive the electric vehicle and cross to the "charging" rod which sets up a series TX coil in the ground, the battery can be charged during the driving. This novel charging method saves much time compared to the traditional charging method.

In the field of bio-implants, previously, most biomedical charging devices need cable, which means the conventional devices cannot be designed as compacted and wholly implanted into the human body because of this limitation of charging. However, as the wireless power transfer technology development, this new method gives an opportunity for implanted biomedical devices. It can make the implanted biomedical devices entirely embedded into the human body and recharge the devices without cord [8]-[10]. Due to this technology, the implanted devices can be designed to be very small and embedded into the human body for a whole life without taking out for charging.

Overall speaking, the market for WPT is vast and rapidly growing. The WPT market is expected to reach a total of $15.2 billion in 2020 [11].
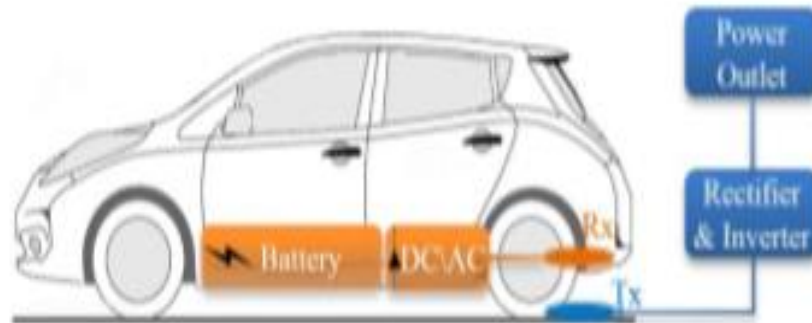
Figure 1.1 EV basic wireless charging concept [6]
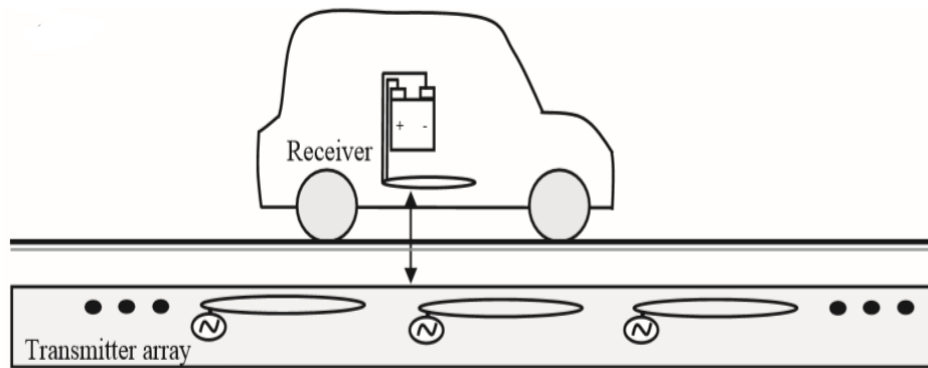
Figure 1.2 EV charging with TX array [7]

1.2 Overview of research status of WPT technology

1.2.1 Research history of WPT technology

The study of wireless power transfer (WPT) technology began in the 1880s, American scientist Nikola Tesla conducted the first WPT experiment. Thereafter, researches on wireless power transfer began [12]. In the early 1960s, W. C. Brown had done a lot of researches on WPT, which laid the foundation of its experiment and made this concept a reality [13]. In 1968, American aviation engineer P. E. Glaser [14] proposed using the microwave to transmit power from the solar satellites to the ground, namely the establishment of space solar power stations (SPS) in geosynchronous orbit. In the following 1977-1980, the U.S Department of Energy and National Aeronautics and Space Administration (NASA) jointly organized a study to demonstrate the concept of the SPS plan and confirmed its feasibility. In response to the global energy crisis, the central developed countries, such as America and Japan, have carried out the study of space solar power, which significantly promoted the development of WPT technology [15]-[16]. In the 1990s, J. T. Boys and others at the University of Auckland in New

Zealand conducted thorough research on the WPT technology and firstly proposed the Inductively Coupled Power Transfer (ICPT) technology [17]. Since the beginning of the 21st century, WPT technology research has made breakthrough progress. In 2007, Marin Soljacic used the magnetic coupling resonant principle to realize the transmission of medium-range radio energy and light a 60 W bulb in more than 2 m distance with a transmission efficiency of about 40% [6]. In recent years, researchers from all over the world have made an in-depth study on WPT and have made significant progress in theory and practice.

1.2.2 Comparison of the advantages and disadvantages of several typical WPT technology

According to the different transmission mechanisms, WPT technology can be divided into magnetic field coupling, microwave radiation, laser emission, electrical-field coupling and ultrasonic transmission type, etc. According to the distance from the source, it can be divided into the near-field coupling and far-field. The magnetic field coupling includes magnetically-coupled inductive and magnetically-coupled resonant, which with the electric field coupling belong to the near-field coupling type. The microwave radiant and laser emission belong to far-field type. Due to these two groups are categorized by the distance or air gap of the transmitter and receiver coils. So, if the wavelength of the wave signal is smaller than the transfer distance, it can be consider as far filed technology. However, if the signal wavelength is larger than transmission distance, it is near field technology. Far field transmission or radiative transmission can always transfer the energy over a long distance with electromagnetic wave. While the system efficiency

4

is lower than near field method because of the radiative power emission's omnidirectional nature. But the transfer frequency band is quite wide, from GHz to THz. The near field techniques can deliver high power with high efficiency. Nevertheless, it is sensitive to the distance various and only can achieve the high power transfer in short distance.

Magnetically-coupled inductive WPT (MCI-WPT) technology is the oldest power transfer technology, which is still widely used now. During the inductive coupling transmission, the power passes through two coupled coils by the magnetic field. This mode of power transmission is similar to the transformer as shown in figure1.3 and figure1.4. Moreover, the inductive coupling technique is the only method applied to commercial products [18]. The transmission power depends on the mutual inductance M, $M = k/\sqrt{L1L2}$, where K is the coupling factor. L1 and L2 represent the two power transfer coils value, separately. The energy crosses the first coil and couples to the second coils. However, the distance between these two coils is not always fixed. And the power transfer efficiency and power delivered to the load are influenced by the distance and misalignment of the two coils, L1 and L2. So, how to decide the distance and misalignment for the two coils is crucial when designing the traditional wireless power transfer system.
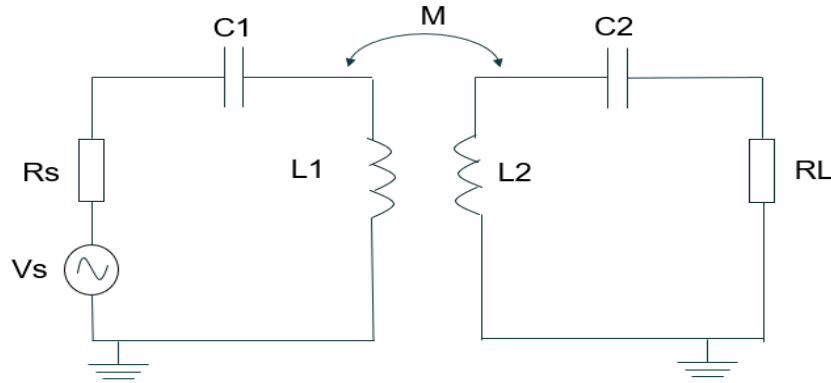
Figure 1.3 Topology of WPT system

Magnetically-coupled resonant becomes the most recommended method in wireless power transfer system since it's discovered by scientist Marin Soljacic of Massachusetts Institute of Technology [18]. The main concept of magnetically-coupled resonant WPT is based on the principle which if the coils of both sides of transmitter and receiver are highly resonant, the magnetic field generated by oscillating current of first coil which is connected to high frequency source, relatively slowly is vanished over very many cycles and in this situation, if a second coil is brought near it, the coil can pick up most of the energy before it is lost, even if it is some distance away. Basic structure schematic diagram of MCR-WPT is shown in Figure. By using this technology, the power can be transferred for a greater distance because this method has high power exchange rate and high Q factor resonator. Although resonant inductive coupling has a high energy transmission rate merit, the drawback is also unique. When the two resonators close slightly tightly, the system resonant frequency becomes unstable and the frequency appears splitting phenomenon. At the original resonant frequency, the load power reduces a lot while the maximum load power will be achieved at the other two new

frequencies. So, if the system wants to achieve maximum power delivered to the load, the system's natural frequency should be tuned to one of the two new frequency points.
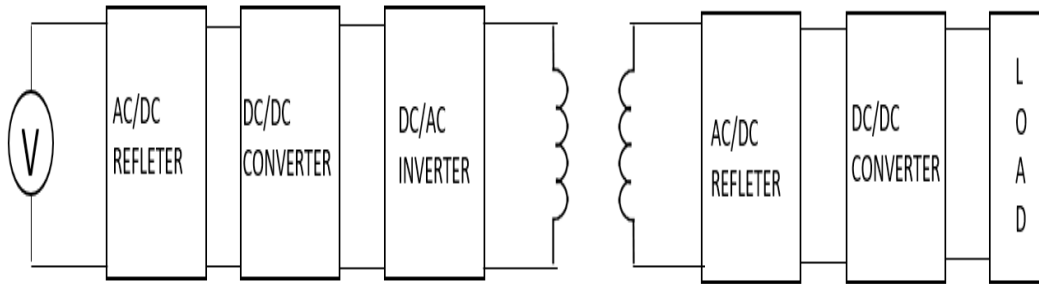
Figure 1.4 Block diagram of wireless power transfer system

Microwave radiation WPT is a far-field wireless power transmission technology. The working principle of microwave radiation WPT is that the microwave power generator converts the direct current power into microwave power and transfers the power effectively to the rectifying antennas by transmitting antennas after focusing the energy. Then, the microwave power is transmitted to the rectifying antenna through free space, and the energy is converted into DC power through the rectification and filtering circuit to supply the loads [19]. Depending on the antenna size, transmitting power, as well as the propagation environment, microwave radiation WPT may achieve power delivery over distances varying from a few meters to even hundreds of kilometers. It has a long the transmission distance, the loss of atmosphere in the process of transmission is less. This technology is relatively mature, but the microwave divergence angle is large, and the power density is low.

The working principle of the laser emission WPT is a laser emission module sends out the specific wavelength of the laser. The laser beams are focused and collimated by the optical transmitting antenna, then launch and arrive at the receiver

through free space, and through the visual receiving antenna focus on photovoltaic modules complete laser-electric energy conversion. The transmission module controls the direction of a laser beam emission and makes the light beam, and the photovoltaic panels are incident to achieve the highest efficiency of photoelectric conversion [20]. The benefit of laser power transfer system is that it achieves long-distance transmission and merely without power loss. However, Laser radiation hazardous for humans and animals. The impact of natural environment also could cause 100% loss during the transmission, for example, atmospheric absorption, fog, etc.

A comparison of the advantages and disadvantages of several typical WPT technology is listed in Table 1.1.

Table 1.1 Comparison of different WPT technologies

Technology	Transmission Range	Frequency	Benefit/ Drawback
Magnetically-coupled inductive WPT	A few millimeters to tens of millimeters	Hz to MHz	High efficiency but short range
Magnetically-coupled resonant WPT	Several centimeters to hundreds of cm	KHz to MHz	High efficiency but frequency splitting
Microwave radiation WPT	Hundreds of meters to thousands of meters	MHz to GHz	Long distance transmission but safety and health issue
laser emission WPT	Tens of meters to thousands of meters	THz	Compact size, high energy concentration but safety and health issues

1.3 Research progress on magnetically-coupled resonant WPT technology

Among the above mentioned of several typical WPT technologies, magnetically-coupled resonant WPT technology has more merits: delivering higher power at longer ranges and with more efficiency, non-radiative, and penetrability one of the research hotspots by the domestic and international scholar. Although the progress of technology in wireless power transfer via coupled magnetic resonances in the last few years is remarkable, there are more problems unsolved. Because the research work of this paper mainly focuses on this technology, hence, in this section, progress and the critical issues in the research on magnetically-coupled resonant WPT technology will be discussed.

In 2007, MIT made a new theoretical breakthrough on wireless power transfer by using a non-radiative electromagnetic energy resonant effect, which successfully lit up a 60 W bulb in 2 m [21]. This technology uses electromagnetic resonance technology, breaking through the previous transformer inductive power transfer mode, with characteristics of high efficiency, long distance, big power, but little dependence on media, opening up a new topic for the medium range (meter-scale range) in wireless power transfer. This technology quickly became the hot pursuing topic for research institutions in recent years. Recently, although some colleges and research institutes have already achieved some meaningful results in terms of magnetically-coupled resonant WPT, which mainly included the topics of system architectures, frequency splitting, impedance matching methods, optimization designs and practical applications, and etc. On the whole, it seems the research is still in its infancy, the following highlights of the research achievements in the aspect of system performance improvement and practical applications.

In the aspect of system performance improvement, to improve power transfer efficiency further, some scholars focused on changing the parameters of the resonator coils [22]-[23] by increasing the radius of the conductor, or using multi-turn wire coils and so forth; other scholars attempted to study and design different resonance compensation topologies to achieve maximum transfer efficiency. Mizuno et al. [24] proposed the use of magnetoplated wire to improve transfer efficiency. Magnetoplated wire is actually a copper wire whose circumference is plated with a magnetic thin film. Thus, the resistance caused by the proximity effect will decrease. Wang et al. [25] analyzed the equivalent circuits and power transfer capacity of various topologies based on inductive coupling mode, but their models are not precise enough due to the ignorance of parasitic parameters of coils in HF. In [26], an alternative method is proposed where the RF power source is replaced by a parity–time symmetric circuit incorporating a nonlinear gain saturation element. However, the circuit's operating frequency varies as a function of the coupling factor, resembling the same drawback of the frequency tuning method. In addition, Zhang et al. [27] propose combining the electric and magnetic coupling to suppress the frequency splitting phenomenon. However, the variation in the power delivered to the load is significant, and the structure of the proposed resonators is complex.

In the aspect of practical applications, magnetically-coupled resonant WPT technology has been reported to be applied in medical implantation, consumer electronics, transportation fields, because of its mid-range, non-radiative, and high-efficiency merits [28]-[45].

In medical implantation applications, batteries are necessary because the micro-system implanted in an organism needs to be powered. However, battery charging or replacements will cause additional economic burden and physical pains on patients. Fortunately, magnetically-coupled resonant WPT technology is appropriate to solve this tough problem. Chang et al. [28] pointed out that batteries can be replaced by this novel technology, the energy for implantable devices can be supplied wirelessly. Li et al. [29] proposed a wireless energy transfer system which is designed and implemented for the power supply of micro-implantable medical sensors, and the volume of the whole implanted part is pretty small.

In the consumer electronics applications, in 2008, based on MIT magnetic resonant technology, Energy transfer device developed by the research team of Seattle Laboratory of Intel with 60W electric energy transferred within one meter, can charge notebook or PDA electrical appliances, and transfer efficiency of 75% has been achieved [30]. In 2009, a wireless charging system based on magnetic resonant was successfully developed by Nagano wireless Co. Ltd in Japan, with a transfer efficiency of 90% within 60 cm [31]. Kim et al. [32] designed a suit of power supply system for LED TV, the operating frequency, transfer efficiency and transfer power are 250 kHz, 80% and 150 W, respectively. Since the 1990s and 2000s, wireless charging technology for portable electronic devices has reached the commercialization stage through the launch of the "Qi" standard by the Wireless Power Consortium, now comprising over 135 companies worldwide.

In the transportation fields, wired charging for power batteries may be dangerous and inconvenient. Fortunately, this charging process can be simplified by WPT [33]-[36].

Except for this stationary charging, dynamic charging (or roadway-charging) attracts more and more attention. This concept was first proposed in the early 1970s [37]. At present, the commercialization processes of this charging technology have been started in many countries, such as Korea, the USA, the UK, and Germany. In summary, wireless power charging for electric vehicles is a promising technology, which is also supported by many companies, including Volvo, Citroen, Evatran, Witricity, Halo IPT, etc.

Although active progress has been made in the research and application of magnetically-coupled resonant WPT technology, there are some critical problems that mainly include the sensitivity of system parameters change, different loads identification, multiple loads impedance matching, electromagnetic environment security, and electromagnetic compatibility. Furthermore, the magnetically-coupled resonant system has the phenomenon of frequency splitting when some parameters (such as resonant coil inductance, equivalent capacitance, and distance between resonant coils) of resonance system changed, the transmission characteristics of the system also changed obviously. In practical application, the magnetically-coupled resonant system often supplies for different loads or multi loads. At this time, the system is required to realize impedance matching well to ensure the system has an excellent performance. In addition, there are still some problems that need to be solved in practical applications, such as whether the electromagnetic environment security can meet the safety standards of the World Health Organization when the magnetically-coupled resonant system works, and how electromagnetic interference influence of the electronic equipment in the surrounding environment, and the anti-interference ability of WPT systems, etc.

1.4 Statement of problem

In recent years, wireless power transfer technologies (WPT) have been growing hot topics for researchers. WPT applications can be found in a wide range from implanted biomedical devices, consumer electronics chargers, and vehicle battery charges [1]-[3]. Among WPT technologies, the magnetic resonance coupling method has a better promise because of its long transfer distance and high efficiency. However, in the Design of magnetic resonance coupling WPT systems, there are still many problems to be solved, such as frequency splitting, prone to efficiency degradation as the operating condition changes, difficulty in maintaining a constant coupling factor between the two coils、limited dynamic range of rectifiers and so on. Among the problems mentioned above, the most critical is frequency splitting. This problem will become more severe as the quality factors of the resonators increase, which is often necessary for achieving high transfer efficiency over long distances. However, it is often difficult to maintain a constant coupling factor in practical applications. The frequency splitting problem will directly affect the transmission efficiency of magnetic resonance coupling WPT systems, which has become the biggest bottleneck hindering the application and promotion of magnetic resonance coupling WPT technology.

Magnetic resonance coupling WPT technology is a cutting-edge topic in the international wireless transmission field at present, which is at the stage of essential theory and experimental research. How to solve the frequency splitting problem and improve transmission efficiency of magnetic resonance coupling WPT systems are related to broad application and promotion of this technology.

Although at present many scholars have done some useful exploration research workaround on how to solve the frequency splitting problem and furtherly improving transmission efficiency of magnetic resonance coupling WPT systems, microscopic researches are working on magnetic resonance coupling WPT technology. In addition, the seldom of studies give detailed analysis on how the splitting frequency changes and what the relationship of the splitting frequency to main circuit parameters is.

The research work of this paper is the theoretical connotation of magnetic resonance coupling WPT technology and certain academic significance and practical value.

1.5 Thesis outline

This paper analyses the frequency splitting phenomenon of the wireless power transfer system, discusses the duffing resonator circuit and its properties, and designs a kind of high-efficiency wireless power transfer inductive system with both non-linear inductors and non-linear capacitors. The main research content of this paper is as follows:

Chapter 1 presents the characteristics, application, and classification of WPT technology. The research status and trend of WPT technologies are overviewed. On this basis, the key problems to be solved for the magnetic resonance coupling WPT technology are brought out.

Chapter 2 studies the frequency splitting phenomenon for the wireless power transfer system. By simulated in ADS, frequency splitting results of the WPT system during the wireless power transmission are studied, and the frequency splitting suppression method is proposed. The above research work provides a theoretical basis for

solving the problem of frequency splitting and designing a kind of high-efficiency WPT system.

Chapter 3 describes the duffing resonator circuit with the nonlinear capacitor, which can eliminate the frequency splitting and keep the high transmission efficiency and power delivered to the load. With the help MATLAB software, the properties of the duffing resonance circuit are discussed. This research work lays a reliable theoretical basis for designing a high efficiency non-linear wireless power transfer system.

Chapter 4 designs a high amplitude non-linear wireless power transfer system based on non-linear inductors with ferromagnetic thin film core and non-linear capacitors with ferroelectric thin film dielectrics based on the above research work. The performance of this system is discussed. The reason for high amplitude of the system is to clarify furtherly.

Chapter 5 summarizes all the works completed from this dissertation and points out future research directions.

CHAPTER 2

FREQUENCY SPLITTING PHENOMENON ANALYZE FOR

WIRELESS POWER TRANSFER SYSTEM

Frequency splitting is an important phenomenon related to transmission efficiency (TE) and WPT capability within the over-coupled region. With the increases of the coupling coefficient, the power transferred to load drops sharply. The resonant frequency splits from one into two within the splitting region. Frequency splitting phenomena have an important influence on the transfer power of magnetic resonant coupling WPT. As a hot research spot, frequency splitting has been actively investigated [46]-[56]. In [46], the directional coupler-based method was suggested to track the splitting frequency in a magnetic resonance system. Reference [47] applied a root locus method to explain the double voltage-peak of frequency splitting of WPT systems. In [48], an asymptotic coupled-mode theory method has been used to analyze the frequency splitting phenomena in contactless power transfer systems. The critical coupling coefficient has been derived based on the energy equations. In [49], a precise analysis of the frequency splitting of the symmetrical and unsymmetrical contactless power transfer systems is shown in detail. However, the studies seldom give a detailed analysis of how the splitting frequency changes and the relationship between splitting frequency and main circuit parameters.

This chapter mainly studies the frequency splitting phenomenon for the wireless power transfer system. The law and the cause of frequency splitting are discussed. By simulation, frequency splitting problems for the WPT system during wireless power transmission are analyzed; Finally, the frequency splitting suppression methods are proposed. The above research works provide a theoretical basis for solving the problem of frequency splitting and designing a kind of high-efficiency WPT system.

2.1 Frequency Splitting Phenomenon

The frequency splitting phenomenon is a significant characteristic in the inductive coupled wireless power transfer system. When the distance between the two sperate coils decreases, the power transfer efficiency, PTE, and output power at the original frequency point reduces tremendous and the maximum PTE and P_L will be achieved at two new frequency points, figure2.1. Also, with the decreasing coupling distance, the coupling factor value increases at the same time and exceed the critical coupled value, the load power is dropped sharply at the original resonant frequency.

Since the distance between the two coils is not easily fixed in the real applications. Even a small distance various will change the system power transmission. There are three situations of the coupling in the inductive wireless power transfer system: over coupled range, critical coupled range, and under coupled range. When the system is in a different range, the power transmission situation is different. In the under coupled range, the distance of the two circuits is quite large. Under this case, the coupling is really weak, the amplitude-frequency of the system has one peak, and the signal coupling is insufficient. So, the output signal is weak, and the bandwidth is small. Therefore, usually,

when we design the WPT circuit, people do not consider this situation. The ideal situation of the inductive coupling wireless power transfer system is the coupling factor precisely at the critical coupling point. In this situation, the two resonant circuits have the best coupling signal, small signal loss, high loop gain, and reliable output signal. The amplitude-frequency characteristic of the system has a single-peak state, and the bandpass characteristic of the system is better. During the critical coupled range, the receiver side circuit has the largest current, and load power and the PTE are highest. However, during the real application, the distance of the transmitter and receiver is varied. So, the coupling factor is hard to fix at the critical coupling point. The coupling factor value always larger than the critical coupling factor value. Therefore, this complicated situation happens frequently in an over-coupled situation. During this situation, the system amplitude-frequency response appears two peaks appearance. As the coupling coefficient increases, the double-peak characteristic becomes more and more serious in figure 2.1. When the critical coupling factor K increase, the output power decreases at the original frequency point. The circuit cannot obtain the ideal single-peak characteristic by adjusting the resonance frequency of the resonance circuit.
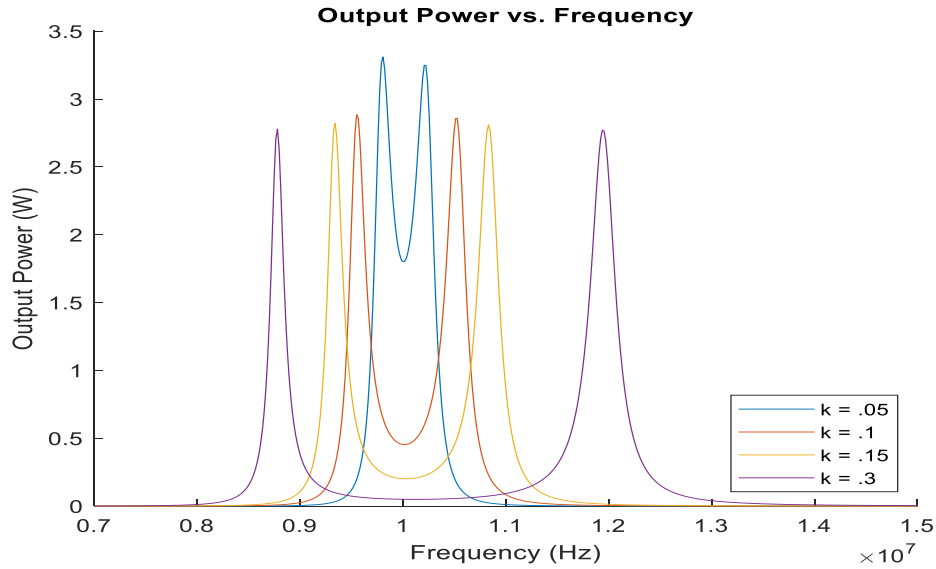
Figure 2.1 Frequency splitting phenomenon in two coils WPT system

2.2 Analysis of frequency Splitting Phenomenon for wireless power transfer system based on equivalent model of mutual inductance

There are two kinds of theoretical models of magnetically-coupled resonant WPT presented. One, based upon coupled-mode theory (CMT) [57]-[58], a perturbation theory, directly analyzes energy coupling between objects by avoiding the complex physical model. The other carries out the theoretical analysis by building up the system physical model and setting the internal equivalent parameters. We adopt the second one for our analysis in this paper.

According to the magnetic coupled wireless power transfer technology's correlation theories, the wireless power transfer system is composed of two resonance inductors L1 (transmitting coil) and L2 (receiving coil). By setting relevant parameters,

the two resonant coils manage to remain in their own resonant state so as to achieve

strong energy coupling.
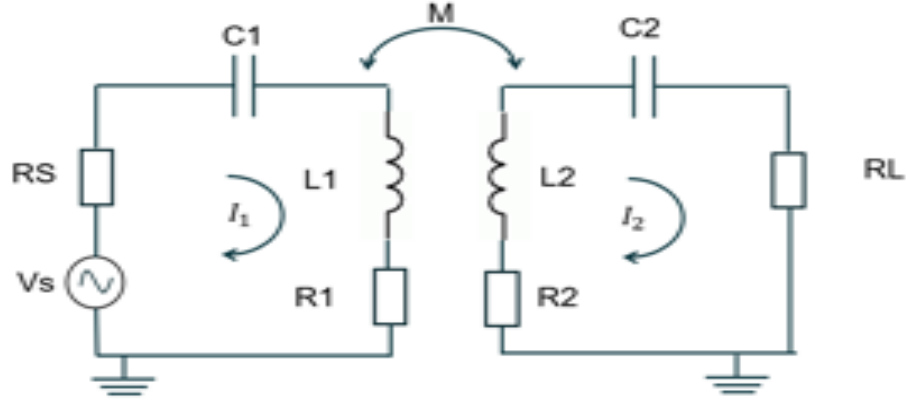
Figure 2.2 Conventional two coils CPT system

Contactless power transfer is known as the CPT system or wireless power transfer

system which is composed of two shot range resonant coils systems. The CPT structure is

shown in Figure2.2.

In figure 2.2, Vs, R_S, L_1, C_1, R_1, R_2, C_2, L_2, and R_L represent power, source inner

resistor, primary side inductor, transmitter side capacitor, loss resistance of primary coils,

loss resistance of the secondary coil, receiver side capacitor, secondary-side inductor, and

load, respectively. M is the inductive coupling between the transmitter and receiver coils.

According to the KVL of circuit theory, we can obtain the following equation.

$$V_S = Z_T I_1 + j\omega M I_2 \qquad (2\text{-}1)$$

$$0 = j\omega M I_1 + Z_R I_2 \qquad (2\text{-}2)$$

Where Z_T and Z_R stand for the impedances of primary and secondary coils

respectively. $Z_T = R_S + R_1 + j(\omega L_1 - 1/\omega C_1) = R_T + jX_T$, $Z_R = R_L + R_2 +$

20

$j(\omega L_2 - 1/\omega C_2) = R_R + jX_R$. ω is the angular frequency. I_1 and I_2 are the transmitter

resonant circuit and receiver resonant circuit currents, respectively. According to

equation 2-1 and 2-2, the equivalent currents of two coils can be obtained.

$$I_1 = \frac{Z_R V_S}{Z_T Z_R + (\omega M)^2} \tag{2-3}$$

$$I_2 = \frac{-jV_S \omega M}{Z_T Z_R + (\omega M)^2} \tag{2-4}$$

Then the power transferred from the primary coil to the secondary coil can be

expressed as:

$$P_L = \frac{\omega^2 M^2 V_S R_L}{(\omega^2 M^2 + R_T R_R - X_T X_R)^2 + (R_R X_T + R_T X_R)^2} \tag{2-5}$$

Alone with the coupling factor increasing, the maximum power delivery to the

load split from one peak into two peaks at two different frequencies. And they are formed

into two modes. The lower frequency point peak is the odd mode, and the higher

frequency point peak is even modes. The load power is related to the partial derivative of

itself. So, the load power P_L derivates M and the value of the derivates function equal to

zero.

$$\frac{\partial P_L}{\partial \omega} = 0 \tag{2-6}$$

The name of this equation is splitting equation [59].

$$\omega^2 M^4 + \omega^2 \frac{dP_a}{d\omega} M^2 + P_a \frac{dP_a}{d\omega} + P_b \frac{dP_b}{d\omega} - \frac{1}{\omega} P_a{}^2 - \frac{1}{\omega} P_b{}^2 = 0 \tag{2-7}$$

In equation 2-7, P_a and P_b are $P_a = R_T(R_L + R_R) - X_T X_R$ and $P_b = R_T X_R + (R_L +$

$R_R)X_R$, respectively. In order to simply calculation, primary and secondary part of circuit

component parameters are kept same. $R_X = R_R = R$, $C_1 = C_2 = C$, and $L_1 = L_2 = L$,

when the load power reaches extremum, solving the solution of quadric equation of M of

source angular frequency.

When M<$M_{critical} = \sqrt{-C^2\left[R^4 - 4\frac{L}{C}R^2\right]/4}$, the solution only has one solution.

$$\omega_{weak} = \sqrt{\frac{(R^2-\frac{L}{C})+\sqrt{(R^2-2\frac{L}{C})^2+\frac{12}{C^2}(L^2-M^2)}}{2(L^2-M^2)}} \qquad (2\text{-}8)$$

When M>$M_{critical}$, the equation has two maximum solutions.

$$\omega_1 = \sqrt{\frac{(R^2-\frac{L}{C})+\sqrt{(R^2-2\frac{L}{C})^2+\frac{4}{C^2}(L^2-M^2)}}{2(L^2-M^2)}} \qquad (2\text{-}9)$$

$$\omega_2 = \sqrt{\frac{(R^2-\frac{L}{C})-\sqrt{(R^2-2\frac{L}{C})^2+\frac{4}{C^2}(L^2-M^2)}}{2(L^2-M^2)}} \qquad (2\text{-}10)$$

When M=$M_{critical}$,

$$\omega = \sqrt{\frac{-(R^2-2\frac{L}{C})}{2(L^2-M^2)}} \qquad (2\text{-}11)$$

$M_{crtical}$ is a critical coupling point, and there is only one maximum point at one

frequency while the distance between the transmitter and receiver is exactly situated at

the critical distance. Alone with the transmission distance of the transmitter and receiver

become grater, and the mutual coupling M is smaller than $M_{crtical}$. The whole system is at the weak coupling situation, and the largest load power is around frequency ω_{weak}.

When the transmission distance of the two the coils is getting closer which is shorter than the critical transmission distance, M>$M_{critical}$, the system is at over coupled range, and the maximum load power will be split into two points and appeared at ω_1 and ω_2, respectively.

However, when the system situates at weak coupling range, although the load power at ω_{weak} is maximum, compared to the maximum power deliver to the load at over coupled range, the ω_{weak} point load power is smaller than the power at ω_1 and ω_2 points. The ideal situation of the CPT system is M=$M_{critical}$.

2.3 Efficiency, Power Transfer Efficiency, and $|S21|^2$

Efficiency

$$\text{Effciency} = \frac{P_L}{P_{system} - P_{dis\_source}} = \frac{R_L}{(\frac{I_T}{I_R})^2 R_T + R_L - R_R} \tag{2-12}$$

In this equation, P_{system} is whole system power, and P_{dis_source} is disputed power of the power. According to equation 2-3 and 2-4, we can get the $(\frac{I_T}{I_R})^2 = \frac{Z_R^2}{(\omega M)^2} = \frac{(R_L + R_R + jX_R)^2}{(\omega M)^2}$.

X_R=0, ω euqals to $\frac{1}{\sqrt{LC}}$. So, the maximum efficiency is shown below

$$\text{Effciency}_{max} = \frac{(\omega M)^2 R_L}{(R_L + R_R)^2 + (\omega M)^2 \cdot (R_L + R_R)} \tag{2-13}$$

As shown in equation 2-13, the whole system's maximum efficiency does not have a frequency splitting phenomenon. The resonant frequency of the whole system is the same as the receiver side circuit resonant frequency during any strength of coupling. While the resonant frequency ω keeps the same, as the coupling strength, M, increases, the Effciency$_{max}$ is increased. Otherwise, the Effciency$_{max}$ is decreased when the coupling M decreases.

However, Power Transfer Efficiency, PTE, is completely different with the system efficiency. PTE in [60] is defined as

$$\text{PTE} = \frac{P_L}{P_{av,S}} \qquad (2\text{-}14)$$

where P_L is load power, and $P_{av,S}$ is power available from the source. PTE is similar with transducer efficiency. In the power transfer efficiency definition, the source and load matching has been considered, which means the maximum power can be transferred from the source to the load. However, PTE is also closely related to mutual inductance M, which is the function of the coupling factor. Similar with the P_L, there is also frequency splitting phenomenon for power delivered to the load.
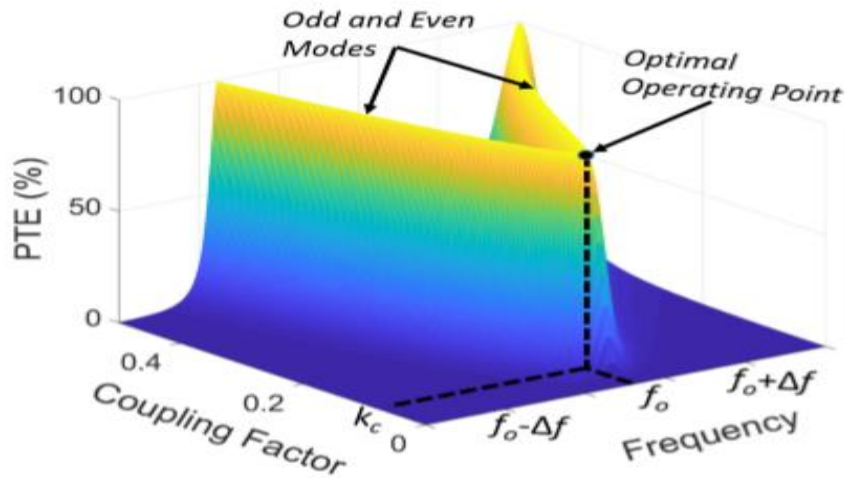
Figure 2.3 PTE versus resonant frequency versus coupling factor of

WPT transfer system [61]

PTE versus resonant frequency versus coupling factor response is given by figure

2.3. In figure 2.3, the coupling factor is inversely proportional to the distance between the

transmit and receive coils. f_0 is the optimal operating frequency point, where the

frequency splitting does not happen, and the maximum PTE is obtained. When the

coupling factor k is less than K_c, $0<K<K_c$, the system frequency still maintains at f_0, but

PTE decreases with K various. During this status, the frequency does not split while the

power transfer efficiency keeps decreasing because the transmitter circuit power cannot

deliver to the receive side through a large gap and weak coupling. Nevertheless, when the

distance of the two coils is getting closer and $K>K_C$, the frequency splitting phenomenon

appears, and the maximum PTE only can be achieved at two different frequency points

which are $f_0 - \Delta f$ and $f_0 + \Delta f$.

At the optimal frequency point, PTE arrives at the maximum point, and the

transmitter and receiver circuits are matched. However, in the real world, the distance and

alignment of the transmitter and receiver coils are difficult to control, for instance, wireless phone charging, implanted biomedical devices charging, and EV charging. It is very difficult to maintain high PTE because it is hard to make the distance between the transmitter coil and receiver coils keeping at the critical distance. Once the distance changes, seriously fluctuation of PTE will happen. How to eliminate the frequency splitting phenomenon and keep high PTE during the over coupled range is currently a hot research topic.

Definition of $|S21|^2$ is the same as the power transfer efficiency. It means the ratio of the power delivered to the load and the power available from source, but the loss of source resistor power is not included. S_{21} is shown in [62]

$$S_{21} = 2\frac{V_L}{V_S}\sqrt{\frac{R_S}{R_L}} \qquad (2\text{-}15)$$

Substituting 2-1 and 2-2 into 2-15, S_{21} and $|S21|^2$ can be deduced below:

$$S_{21} = \frac{2j\omega k\sqrt{L_1 L_2}\sqrt{R_S R_L}}{Z_T Z_R + \omega^2 k^2 L_1 L_2} \qquad (2\text{-}16)$$

$$|S21|^2 = \frac{4\omega^2 k^2 L_1 L_2 R_S R_L}{(Z_T Z_R + \omega^2 k^2 L_1 L_2)^2} \qquad (2\text{-}17)$$

2.4 Design and Simulation of the Proposed Model

After analyzing wireless power transfer circuit, we simulate the conventional two coils wireless power transfer model into ADS, Advance Design System. The schematic diagram is presented in figure 2.4. In this circuit, we design the whole system resonant frequency at 10 MHz. In order to simply the simulation, we make $C_1 = C_2 = 12.67pF$

26

and $L_1 = L_2 = 20uH$. The coupling factor, K, is various during the simulation. By changing the value of K, we can simulate the situations of under coupled range, critical coupled range, and over coupled range. The suggested circuit parameters are provided in Table 2.1. And the three situations' efficiency and S21 of wireless power transfer circuit are shown in figure 2.5 to figure2.10. The coupling factor K in figure 2.5 and figure 2.6 is 0.03 and 0.02, respectively. And they are under under-coupled range. The system is at critical coupled range when the coupling factor is at 0.04, in figure 2.7. The figure 2.8 and figure 2.9 are presented the efficiency and S21 of system at over-coupled range. All the results are performing S-parameters and frequency analysis.

According to the relationship f = F (k23), S21 magnitude against k23 of tuned frequency and fixed frequency is shown in below.
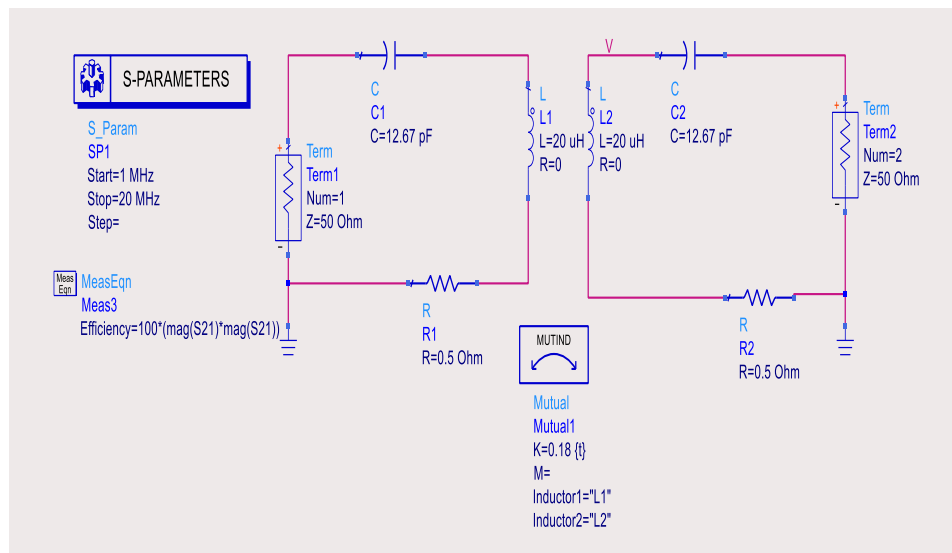
Figure 2.4 Schematic of Two-Resonator-Coil WPT in ADS
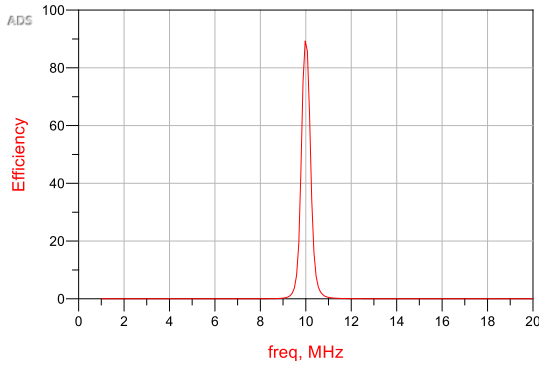
(a)
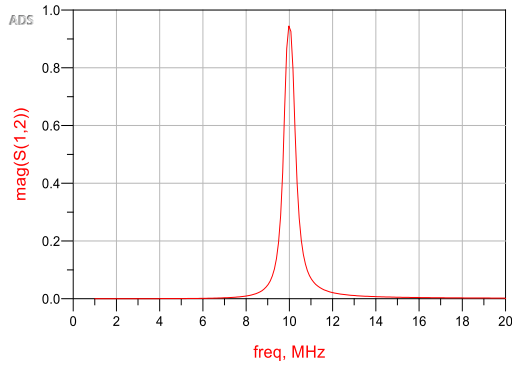
(b)

Figure 2.5 Efficiency and |S21|for WPT at K=0.03 (a) under-coupled range efficiency (b) under-coupled range mag(S21)
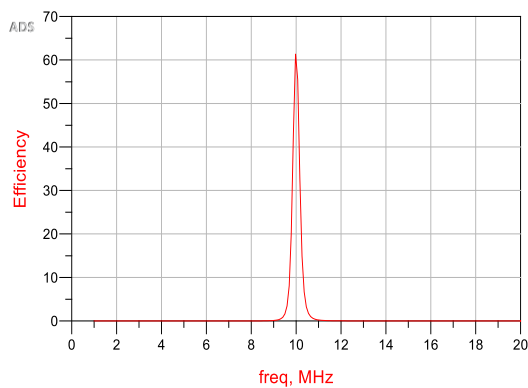
(a)
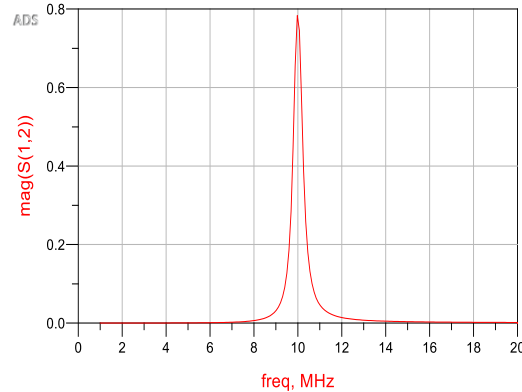
(b)

Figure 2.6 Efficiency and |S21|for WPT at K=0.02 (a) under-coupled range efficiency (b) under-coupled range mag(S21)

The results of the model for the coupling factor at the under-coupled range are shown in figure 2.5 and figure 2.6. When the coupling factor value decreases from 0.03 to 0.02, the efficiency of the system decreases from 90% to 61%. The mag(S21) decreases from 0.95 to 0.79. So, when the system is at under-coupled range, as the coupling factor decreases, the system efficiency decreases. And there is only one peak of the largest efficiency point. The system efficiency decline is caused by the weak coupled

link between the two resonant coils. The power is hard for couple from one side to another.

(a)   **(b)**
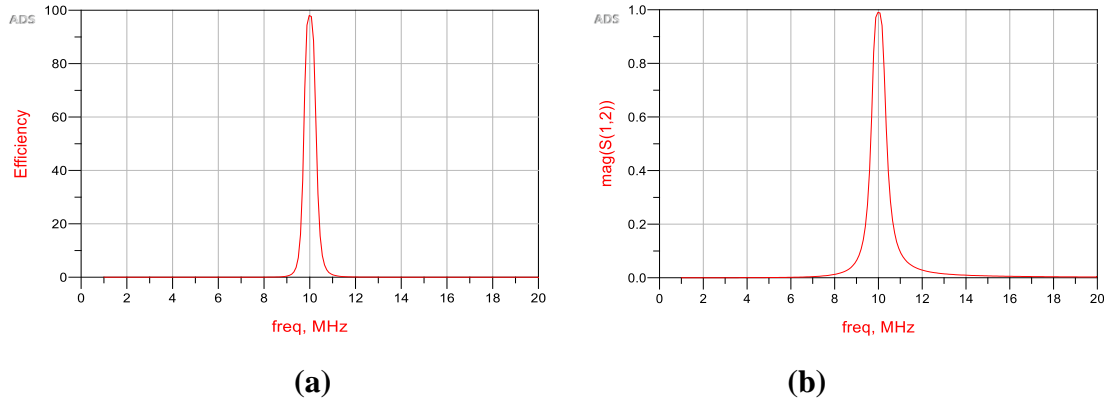
Figure 2.7 Efficiency and |S21|for WPT at K=0.18 (a) critical-coupled range efficiency (b) critical-coupled range mag(S21)

Figure 2.7 showed the system at the critical coupled range when the coupling factor is 0.04. At this point, the efficiency is 100%, and mag(S21) is at 1 while the resonant frequency is 10 MHz. At the critical coupled point, the maximum efficiency only exists at system resonant frequency. There is only one peak in the results.

(a)   (b)
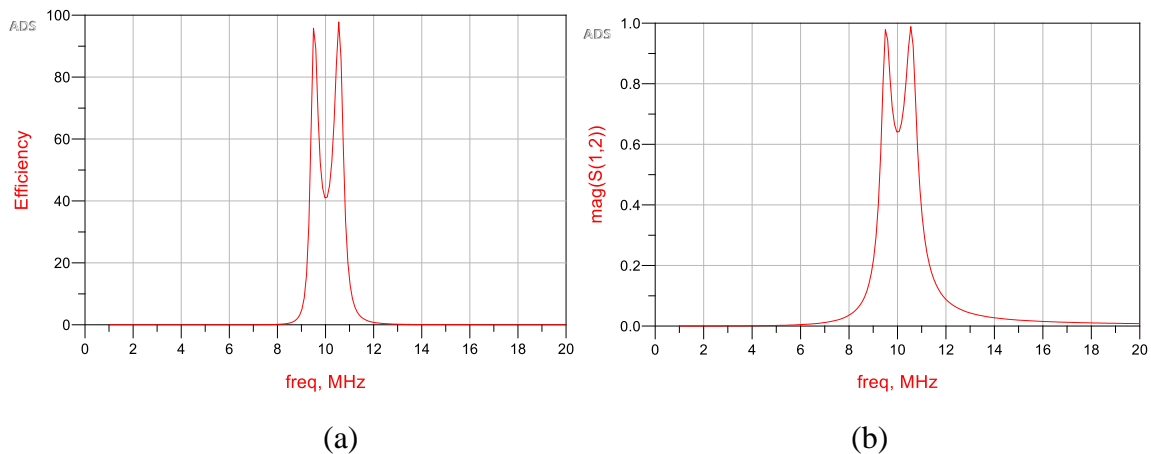
Figure 2.8 Efficiency and |S21|for WPT at K=0.11 (a) over-coupled range efficiency (b) over-coupled range mag(S21)
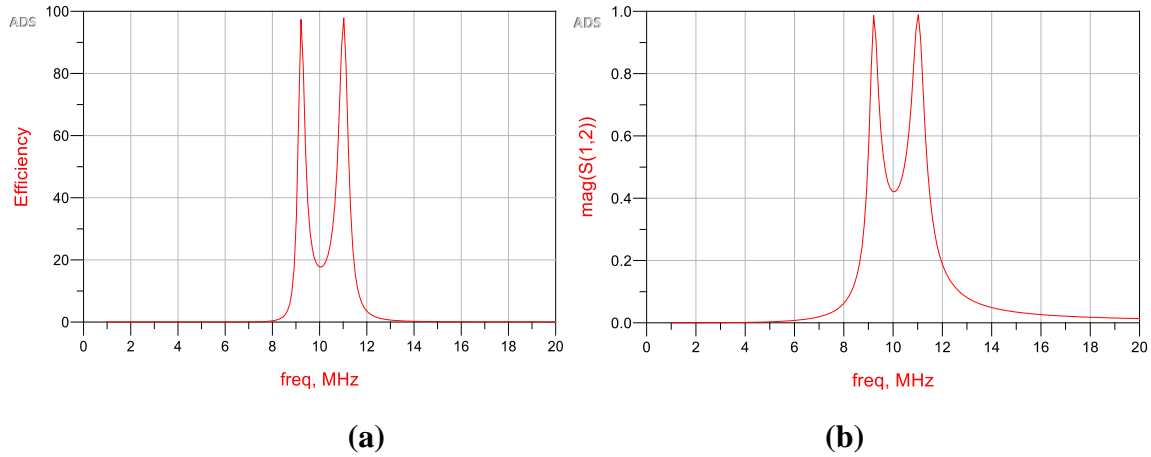
Figure 2.9 Efficiency and |S21|for WPT at K=0.18 (a) over-coupled range efficiency (b) over-coupled range mag(S21)

However, after the coupling factor increases, the maximum efficiency appears frequency splitting phenomenon, as shown in figure 2.8 and figure 2.9. The over-coupled range is between from 0,04 to 1 at this system. When the coupling factor, K, is up to 0.11, the maximum frequencies and mag(S21) emerge at 9.5 MHz and 10.5MHz. When the coupling factor, K, is up to 0.18, the maximum frequencies and mag(S21) emerge at 9.1 MHz and 11MHz. Comparing the results in figure 2.8 and figure 2.9, as the coupling factor increases, the value between the lower maximum frequency point and the larger maximum frequency point increases. At the original frequency point, 10 MHz, the efficiency, and mag(S21) drop deeper and deeper. It means when the system at the over coupled range, the maximum efficiency cannot be achieved at the original frequency point. This is due to the system appears mismatch phenomenon. During this situation, all the power cannot be delivered at a resonant frequency point. But the maximum will achieve at the two new frequency pints and two peaks phenomenon presents. The odd mode and even mode appear, respectively. The lower frequency maximum point is odd mode, and the higher frequency maximum points is even mode.

Table 1.1 Calculated parameters for two-coil WPT system

Parameter	Value
Frequency	10 MHz
$C_1 = C_2$	$12.67 pF$
$L_1 = L_2$	$20\ uH$
$R_S = R_L$	50 Ohm
K (coupling factor)	0-1

2.5 Frequency splitting suppression method

In order to eliminate the frequency splitting phenomenon and achieve maximum efficiency at one frequency point, four commonly used methods for suppression frequency splitting phenomenon are proposed in the previous WPT studies [63]-[69]. The first one is changing the WPT system's structural parameter, which adjusts the coupling coefficient between the power coil and the transmitter coil [63]-[64]. The second method is adjusting the system power supply frequency which means detecting the reflected power or current at the transmitter side and adjusting the system's resonant frequency to reach the resonant frequency again [65]. The third method is designing an impedance matching network. Frequency splitting happens due to mismatch. So, designing a tunable matching circuit [66]-[69] and adjusted capacitors' value can effectively solve this problem. The latter method is designing a transmitting coil that generates a reverse

31

magnetic flux. By designing a transmitting coil composed of two sets of coils that generate reverse magnetic flux and retarding, the rate of change of the coupling coefficient which dues to the change in distance curbs the frequency splitting.

So far, most approaches of suppression frequency splitting phenomenon in the literature need active circuits or active feedback control circuits. Therefore, those designs make the whole WPT system more complete and lose more power. They achieve suppression frequency splitting but introduce more energy loss.

The nonlinear components can provide nonlinear characteristic for the circuit, such as nonlinear capacitor and nonlinear inductor [70]-[73]. The nonlinear characteristic some time could give the circuit unimagined benefits. The new nonlinear passive suppression frequency splitting circuit, duffing resonator, is proposed in [60]. They use duffing oscillator characteristic to eliminate the frequency splitting phenomenon. The author by replacing the linear capacitor to nonlinear capacitor, NC, achieves duffing resonator design. This thesis' design is based on this "duffing" theory. We replace the nonlinear capacitor and nonlinear inductor, NCNL at same time in the circuit. The numerical analysis is presented in chapter 3 and chapter 4.

CHAPTER 3

DUFFING RESONATOR BASED WIRELESS POWER TRANSFER SYSTEM THEORY

Although magnetically-coupled resonant WPT(MCR-WPT) technology has become the mainstream method for wireless power transfer due to its high efficiency, MCR -based systems are prone to efficiency degradation as the operating condition changes. Additionally, as mentioned in Chapter 2, one of the most significant challenges in the design of SCMR WPT systems is its low tolerance to the coupling factor variations because of the frequency split phenomenon. To fundamentally solve the above problems, we investigate a nonlinear resonance circuit described by the duffing equation replacing linear capacitor into the nonlinear capacitor, as well as the properties of the duffing resonator circuit by MATLAB software. This idea is first proposed by Dr. Amir Mortazawi's team.

3.1 Duffing equation was proposed by Georg Duffing in 1918. The basic form of the which is usually written as (3-1) [74]:

$$\ddot{x} + \delta\dot{x} + \alpha x + \beta x^3 = \gamma \cos(\omega t) \tag{3-1}$$

Where x is displacement ,t is the time, δ is the amount of damping, α is the linear stiffness, β is the amount of non-linearity in the restoring force, γ is the amplitude of the periodic driving force, and ω is the periodic driving force angular frequency.

In [64] and [74], the duffing equation is described as:

$$\ddot{x} + 2\gamma\dot{x} + \omega_0 x + \epsilon x^3 = F\cos(\omega t) \qquad (3\text{-}2)$$

Where x is displacement, γ is the damping coefficient, $\omega 0$ is the natural resonant/oscillate frequency, ϵ is the third order nonlinearity coefficient, and $F\cos(\omega t)$ is the excitation with the amplitude F and angular frequency ω.

The steady state solution of 3-2 in [12, 63] is $x(\omega, t) = A(\omega)\cos(\omega t - \theta)$. A is frequency-dependent amplitude and θ is phase difference in reference to the excitation signal. So, the amplitude as function of excitation frequency can be get:

$$A^2\left[(\omega_0{}^2 - \omega^2) + \frac{3}{4}\epsilon A^2\right]^2 + (2\gamma A\omega)^2 = F^2 \qquad (3\text{-}3)$$

The representative amplitude response of a Duffing resonator is shown in figure 3.1 [74]. It can be observed from Fig.3.1 that the frequency response curve of the linear resonator and duffing resonator amplitude are drawn into the same axis, and the duffing resonator response always tilted to one side (right side in this figure). Unlike the frequency response curve of the linear resonator which only has one maximum stable amplitude point, the frequency response curve of the duffing resonator has three distinct root regions (upper equilibrium brunch/point, unstable solution, and lower equilibrium brunch/point) [74]. Among these three root regions, the middle solution point is unstable, while the upper and lower points are stable (called equilibrium points). It can also be

34

observed from figure 3.1 that a steady-state solution of the system converges to the upper

equilibrium point or lower equilibrium point.
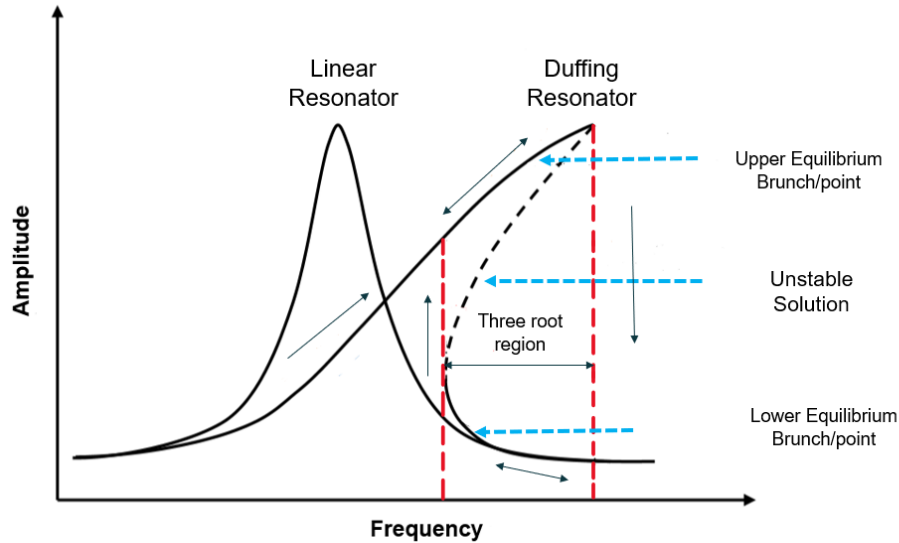
Figure 3.1 The amplitude-frequency responses of duffing resonator and linear
resonator [74]

In addition, it can also be observed from figure 3.1 that the region between the

two red dash lines is an unstable solution, which is very important when the response of

the duffing resonator is analyzed. If the circuit is excited to converge to the high-

amplitude solution point, the amplitude will follow the upper curve when frequency

changes. Once the right boundary of the three-root region is crossed, the amplitude drops,

which is known as a drop-down phenomenon [74]. However, if the circuit is excited to

converge to the low-amplitude solution point, the amplitude will remain the small unless

the three-root region's left boundary (the jump up to point) is crossed. So, when nonlinear

duffing resonator has the same Q with linear resonator, the nonlinear duffing resonator

has more bandwidth.

The direction of the response curve of the duffing resonator is dependent on ϵ as shown as the 3-2 and 3-3. When ϵ is larger than zero, the amplitude-frequency response curve tends to move to the right which is hardening system, shown as figure 3.2. When ϵ equals to zero, the system is linear. However, when ϵ is a negative number, the curve is tended to move to the left.
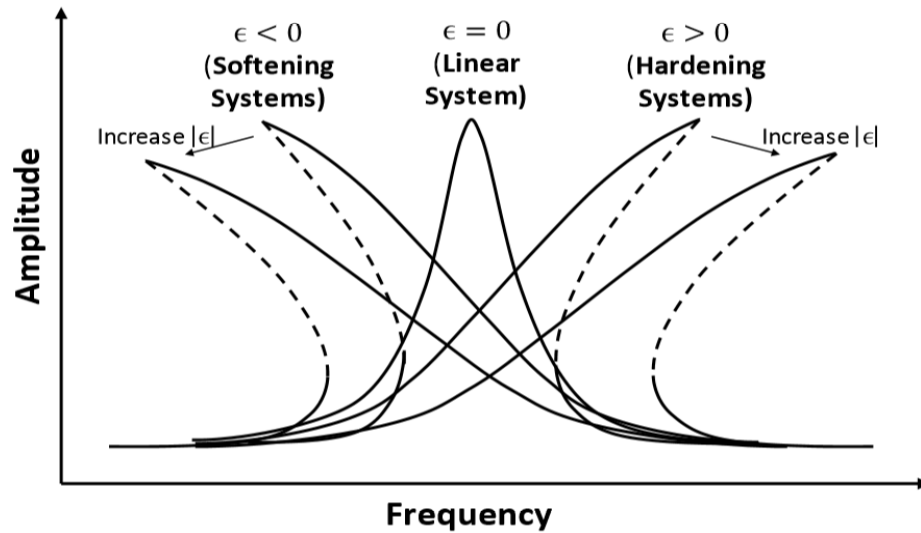
Figure 3.2 The amplitude-frequency responses of duffing resonator with different nonlinearity coefficient ϵ [74].

3.2 Analysis on Nonlinear duffing resonator

After analyzing the characteristic of the duffing equation, we implant this method into a magnetic coupled WPT circuit, as shown in figure 3.3. In figure 3.3, C2 is a nonlinear capacitor. Differently with the traditional WPT circuit, in the nonlinear system, the original linear capacitor of the second circuit has been replaced by nonlinear capacitor C2. The linear capacitor and a sinusoidal excitation voltage $Vs(t) = vs(\omega t)$ still be used in the primary circuit. According to Thevenin's theorem, the coupled wireless power

transfer circuits can be synthesized into one RLC circuit, and the equivalent circuit is shown as figure 3.4. The circuit consists of a voltage source, an inductor, load, and a nonlinear capacitor C.
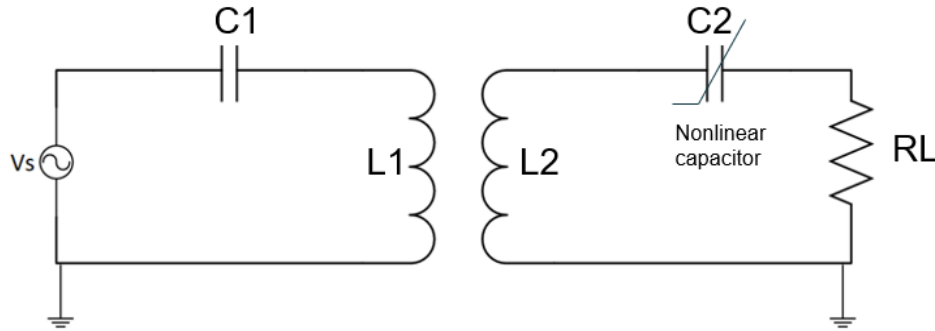
Figure 3.3 Topology of nonlinear WPT system
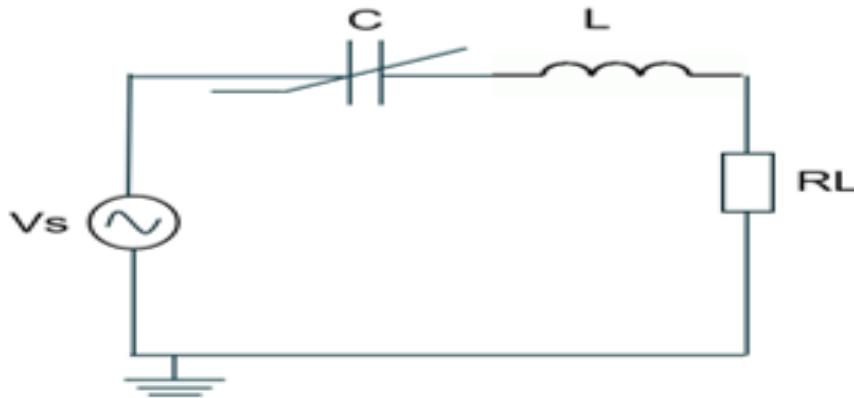
Figure 3.4 Equivalent nonlinear WPT system circuit

The nonlinear capacitor C usually has a symmetric C-V relationship, i.e. $C(V_C) = C(-V_C)$. In the practical circuit design, the nonlinear capacitor with symmetric C-V curve characteristics can be provided with anti-series diode, ceramic capacitors, and ferroelectric varactor devices. BST, barium strontium titanate, based varactor is an

example of ferroelectric varactor diodes. BST varactor displays low loss. In [75], the C-V

response of the BST-based varactor is shown in figure 3.5.

$$C(V) = \frac{C_0}{1+(\frac{4V_C}{3V_2})^2}$$

(3-4)

Where $C = 0.5C_0$ when V_2 is bias voltage. Vc is derived by [76].

$$V_C = \frac{1}{C_0}Q_C + \frac{16}{9V_2{}^2C_0{}^3}Q_C{}^3$$

(3-5)

When the BST-based varactor is used in duffing resonator, a_1 and a_3 equations

presented in 3-6 and 3-7. The C-V curve response of the BST-based varactor with $C_0 =$

100 PF and V_2=5 V is shown in figure 3.5, which is simulated in MATLAB.

$$a_1 = C_0$$

(3-6)

$$a_3 = \frac{9V_2{}^2C_0{}^3}{16}$$

(3-7)
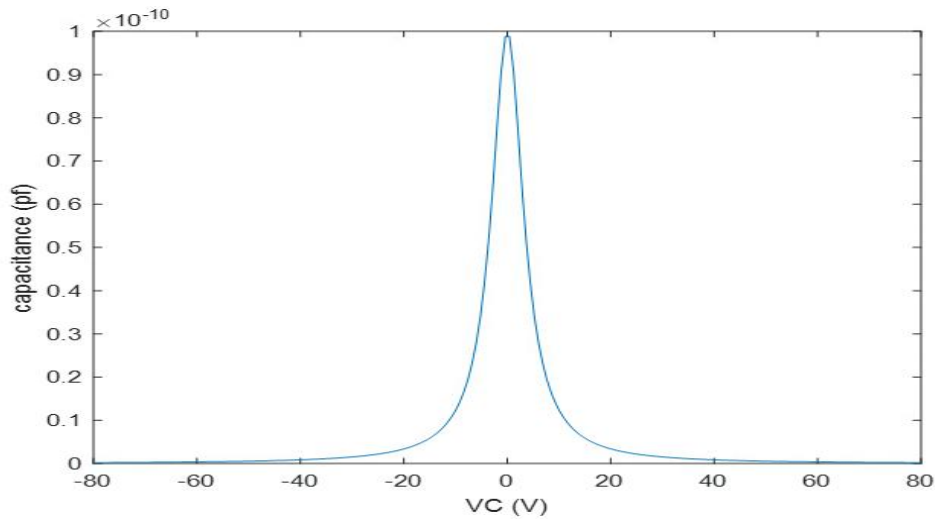
Figure 3.5 Bell shape symmetric C-V curve of BST-based varactor

The dynamic equation of nonlinear wireless power transfer resonator based on Kirchhoff voltage law (KVL) is given as follows:

$$V_C(t) + R\frac{dq}{dt} + L\frac{d^2q}{dt^2} = V_S cos(\omega t) \tag{3-8}$$

Where $V_C(t)$ is the voltage across nonlinear capacitor, and $V_S(\omega t)$ is the source voltage q(t) is the charge amount of the nonlinear capacitor. q is the amount of charge stored in the capacitor which is the function of V_C. So, the charge amount can be expressed as q = f(Vc), and the voltage across the nonlinear capacitor can be furtherly written as $V_C = f^{-1}(q)$. Because the nonlinear capacitor has symmetric bell shape or wall shape C-V relationship, the even order terms of Taylor expansion vanish. The Taylor series expansion can be expressed by:

$$V_C = \frac{1}{a_1}q + \frac{1}{a_3}q^3 + \cdots\cdots \tag{3-9}$$

Neglecting the higher than third-order terms for simplicity, 3-9 can be rewritten as:

$$V_C = \frac{1}{a_1}q + \frac{1}{a_3}q^3 \tag{3-10}$$

Substituting 3-10 into 3-8 results in 3-11:

$$\frac{1}{a_1}q + \frac{1}{a_3}q^3 + R\frac{dq}{dt} + L\frac{d^2q}{dt^2} = V_S(\omega t) \tag{3-11}$$

Comparing equation 3-11 with 3-2, it is found that the forms of these two equations are the same. So, the nonlinear resonator equation 3-11 can be used in a nonlinear RLC resonator, which has the same characteristic with the duffing system. q =

$Q\cos(\omega t - \theta)$ is the solution of 3-11. Q is the amplitude of the charge amount dependent on time. The restoring effect is contributed by both the linear term $\frac{1}{a_1}$ and the nonlinear term $\frac{1}{a_3}$. In order to simplify the calculation, the equivalent liner term is written as [27].

$$\int_0^{\frac{T}{2}}(\frac{1}{La_3}Q\cos(\omega t - \theta)^3)d(Q\cos(\omega t - \theta)) = \int_0^{\frac{T}{2}}(\frac{1}{C_{eff}}Q\cos(\omega t - \theta))\,d(Q\cos(\omega t - \theta))$$

$$(3\text{-}12)$$

From equation 3-12, $Ceff$ can be calculated as 3-13:

$$\frac{1}{C_{eff}} = \frac{\frac{1}{a_3}}{\frac{3}{4}Q^3} \tag{3-13}$$

Substituting 3-13 into 3-11 results in 3-14:

$$R\frac{dq}{dt} + L\frac{d^2q}{dt^2} + \frac{1}{a_1}q + \frac{1}{C_{eff}}q = V_S\cos(\omega t) \tag{3-14}$$

Simplifying equation 3-14:

$$\ddot{q} + \frac{R}{L}\dot{q} + \frac{1}{La_1}q + \frac{1}{LC_{eff}}q = \frac{V_S}{L}\cos(\omega t) \tag{3-15}$$

Thus, the natural resonant frequency ω_0 can be obtained:

$$\omega_0 = \sqrt{\frac{1}{La_1} + \frac{1}{LC_{eff}}} = \sqrt{\frac{1}{L}(\frac{1}{a_1} + \frac{\frac{3}{4}Q^2}{a_3})} \tag{3-16}$$

The natural resonant frequency ω_0 is dependent on the charge amount of nonlinear capacitor Q, which varies with voltage V_C of the nonlinear capacitor. The frequency-domain format of 3-15 can be written as:

$$(j\omega)^2 Q + \frac{R}{L}Q(j\omega) + \frac{1}{L}(\frac{1}{a_1} + \frac{\frac{3}{4}Q^2}{a_3})Q = \frac{V_S}{L} \tag{3-17}$$

where Q is $Qe^{-j\theta}$.

Substituting Q into 3-17 results in:

$$Q^2(\frac{1}{La_1} + \frac{\frac{3}{4}Q^2}{La_3} - \omega^2)^2 + (\frac{R}{L}Q\omega^2)^2 = (\frac{V_S}{L})^2 \tag{3-18}$$
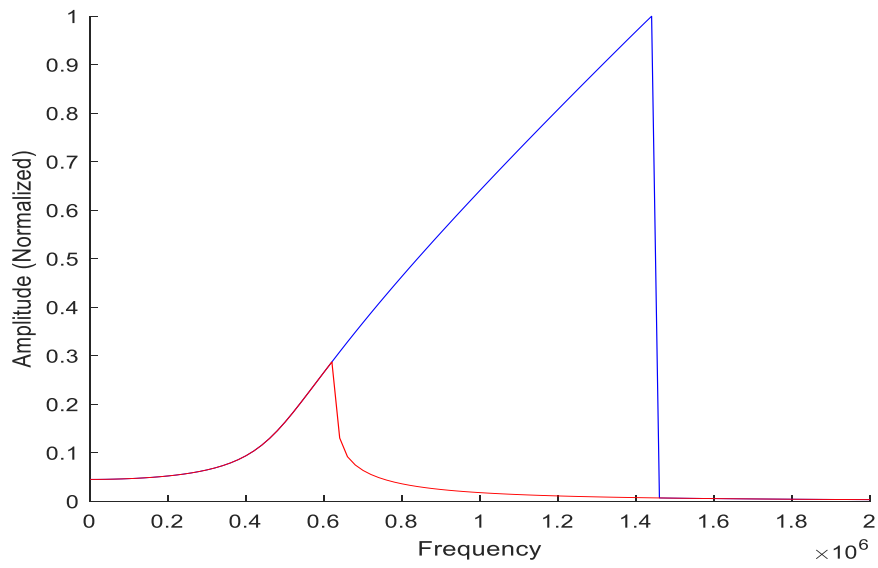
Figure 3.6 Frequency-amplitude response of Duffing resonator circuit
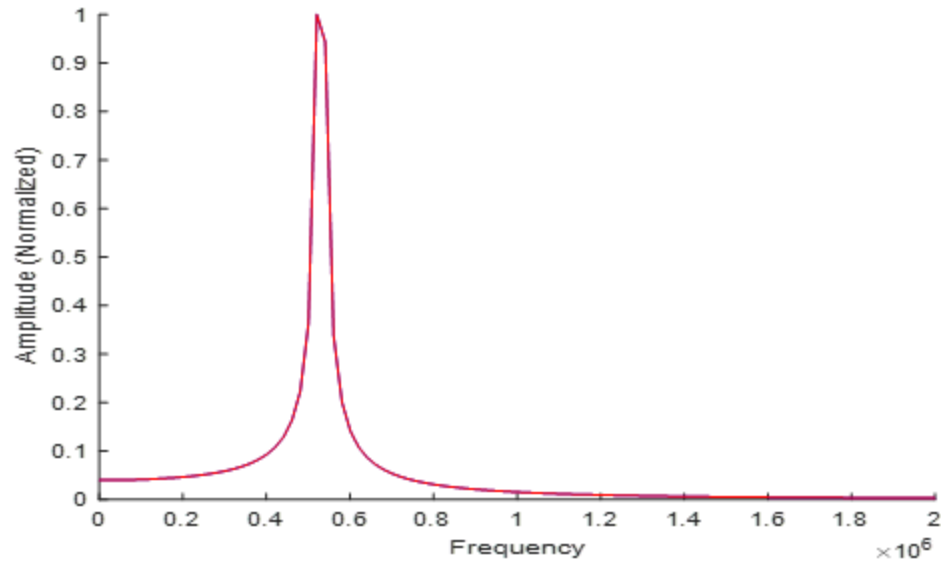
Figure 3.7 Amplitude-frequency response of linear RLC resonator

Based on equations 3-6, 3-7, and 3-18, the duffing resonator with nonlinear capacitor frequency-amplitude response is drawn in figure3.6. The blue curve is the high equilibrium brunch, and the red curve is low equilibrium brunch. Figure 3.7 is the amplitude-frequency response of the linear RLC resonator. Figure 3.6 and figure3.7 has the same Q. In the linear RLC system design, the bandwidth is extremely narrow. The maximum amplitude only can get at a small range. However, nonlinear capacitor duffing resonator ameliorates this situation. The high amplitude bandwidth is enhancement. This difference is caused by the capacitor nonlinear term $\frac{1}{a_3}q^3$.

CHAPTER 4

NCNL DUFFING RESONATOR FOR IMPROVING THE WPT SYSTEM

The research results of the previous chapter have shown that as a very promising solution in designing WPT systems, duffing resonator can not only exhibit a significant advantage in improving the WPT system's tolerance to coupling factor variations without degrading the system's efficiency but also having more wider bandwidth, as compared with the conventional linear resonator.

In order to furtherly improve properties of WPT systems, based on the research work of the previous chapter, this chapter firstly designs a higher efficient non-linear resonator with non-linear ferromagnetic thin film core inductors and non-linear ferroelectric thin film dielectrics capacitors and derives a new of non-linear differential equations governing the non-linear dynamical behavior of the non-linear resonator. Secondly, by numerical simulation, the effects of different parameters on the system behavior are discussed. Finally, the performance comparison between the new system and the duffing resonator mentioned in the previous chapter is compared.

4.1 Analysis of duffing resonator with nonlinear inductor and nonlinear capacitor

In this chapter, we come up with a new "duffing" circuit by replacing the conventional RLC circuit's inductor and capacitor with nonlinear capacitor and nonlinear

inductor. The new equivalent nonlinear WPT circuit with a nonlinear capacitor and nonlinear inductor, NCNL circuit, is shown as figure4.1.
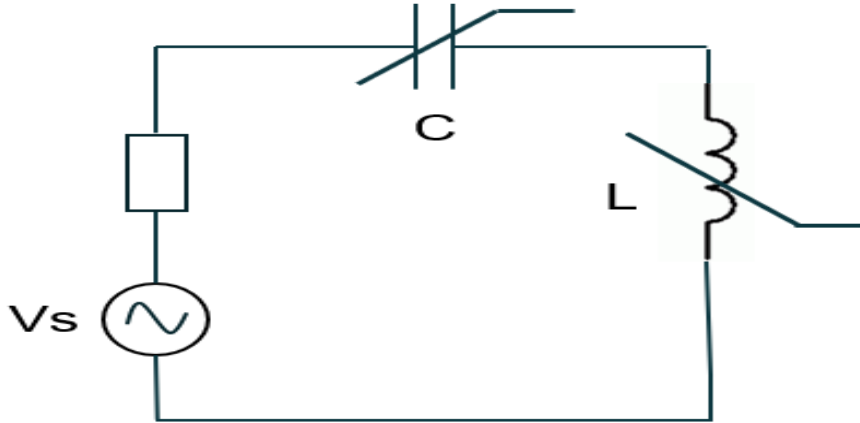
Figure 4.1 New equivalent NCNL circuit

The time-domain dynamic equation of NCNL circuit can be obtained based on the Kirchhoff voltage law.

$$R\frac{dq}{dt} + V_C(t) + V_L(t) = V_S(t) \tag{4-1}$$

Where i $= \frac{dq}{dt}$ and $V_S(t) = V_S\cos(\omega t)$. $V_S(t)$ is the excitation voltage. $V_L(t)$ is the inductor voltage. $V_C(t)$ is the voltage across the capacitor. q(t) is the charger amount into the nonlinear capacitor which is same as q(t) in the chapter 3.

The nonlinear inductor is different from the linear inductor in structure. If the coil does not contain a permeable magnetic medium, it is called nonlinear inductor or air-core inductor. The L of the linear inductor is constant in the circuit and is not be influenced by the applied voltage or current. However, If the coil contains a magnetically conductive medium, such as the inductance L. L will not be constant. It has been called nonlinear

44

inductor. Inductance L is related to the applied voltage or current. The most practical

nonlinear inductor is made by ferromagnetic material. It makes the inductor which has

the nonlinear characteristic. The inductance L(i) of the nonlinear inductor can be

expressed as:

$$\text{L(i)} = L_0 + L_1 i + L_2 i^2 + L_3 i^3 + L_4 i^4 + \cdots\cdots \tag{4-2}$$

Where L_0, L_1, L_2, L_3, L_4, and L_n are the coefficients of L(i). According to the

linear Inductor voltage, the voltage of nonlinear inductor is given as:

$$V_L = L(i)\frac{di}{dt} = \frac{d\emptyset}{dt} \tag{4-3}$$

$$\emptyset = \text{L(i)i} = L_0 i + L_1 i^2 + L_2 i^3 + L_3 i^4 + L_4 i^5 + \cdots\cdots \tag{4-4}$$

Based on the physical characteristic of nonlinear inductor component, we only

consider the odd terms in $\emptyset$ expression, mainly based on consideration as follows: Using

even terms means that the current direction dose not varies with the change of the flux

direction. But, in real life, the direction of the current is varied with the change of

magnetic flux direction. In addition, the even term coefficients are smaller than odd

terms' coefficients. So, in the design, we only consider the odd terms while neglecting

terms higher than the third order in $\emptyset$ expression. The new expression of $\emptyset$ is given as:

$$\emptyset = \text{L(i)i} = L_0 i + L_2 i^3 \tag{4-5}$$

Substituting 4-5 into 4-3, the nonlinear inductor voltage can be obtained:

$$V_L = L(i)\frac{di}{dt} = \frac{d\emptyset}{dt} = \frac{d(L_0 i + L_2 i^3)}{dt} = L_0\frac{di}{dt} + 3L_2 i^2\frac{di}{dt} \tag{4-6}$$

By substituting $i = \frac{dq}{dt}$ expression into 4-6, we have the voltage - q relationship

response of nonlinear inductor as follow:

$$V_L = L_0\ddot{q} + 3L_2\dot{q}^2\ddot{q} \tag{4-7}$$

Substituting 3-10 and 4-7 into 4-1 results in

$$\ddot{q} + \frac{3L_2}{L_0}\dot{q}^2\ddot{q} + \frac{R}{L_0}\dot{q} + \frac{1}{L_0 a_1}q + \frac{1}{L_0 a_3}\dot{q}^3 = \frac{V_S}{L_0}cos(\omega t) \tag{4-8}$$

Equation 4-8 has a similar form with duffing equation 3-1. However, unlike

equation 3-15, this equation has exactly same form with duffing equation. Comparing

with the equation 3-1, the second term in figure 4-8, $\frac{3L_1}{L_0}\dot{q}^2\ddot{q}$, is extra, which is consisted

of the first derivate and second derivate of the charge amount of the capacitor.

$$q = Qcos(\omega t - \theta) \tag{4-9}$$

Where Q is the store charge amplitude in the nonlinear capacitor. θ is the phase

difference with the excitation voltage signal. Although equation (4-8) has a little bit

difference, compared with the conventional duffing equation, we can still use the method

[77].

4.2 Analysis Approach of new NCNL duffing equation

By putting $b_1 = \frac{3L_2}{L_0}$, $b_2 = \frac{R}{L_0}$, $b_3 = \frac{1}{L_0 a_1}$, $b_4 = \frac{1}{L_0 a_3}$, and F=$\frac{V_S}{L_0}$ into equation (4-8) ,

a new equation can be obtained:

$$\ddot{q} + b_1\dot{q}^2\ddot{q} + b_2\dot{q} + b_3q + b_4q^3 = \text{Fcos}(\omega t) \qquad (4\text{-}10)$$

By the new simplified equation 4-10, we can use an approximation method which is called a harmonic balance method, which is used to calculate the steady-state response of the nonlinear differential equation. The excitation voltage can be rewritten as

$$\text{Fcos}(\omega t) = \text{Psin}(\omega t) + \text{Ecos}(\omega t) \quad , \quad F = \sqrt{p^2 + E^2} \qquad (4\text{-}11)$$

and the response expression is

$$q = A\cos(\omega t) \qquad (4\text{-}12)$$

Where A is the amplitude of store charge which is the same as Q in eq. 4-9. Substituting 4-11 and 4-12 into 4-10, we can have the detailed derivation process of equation 4-10 as below:

$$-A\omega^2 cos(\omega t) + b_1(-A\omega sin(\omega t))^2(-A\omega^2 cos(\omega t)) + b_2(-A\omega sin(\omega t))$$
$$+ b_3 A cos(\omega t) + b_4(A cos(\omega t))^3 = p sin(\omega t) + E cos(\omega t)$$

$$-A\omega^2 cos(\omega t) - b_1 A^3 \omega^4 sin^2(\omega t)cos(\omega t) - b_2 A\omega sin(\omega t) + b_3 A cos(\omega t)$$
$$+ b_4 A^3 cos^3(\omega t) = p sin(\omega t) + E cos(\omega t)$$

where

$$cos^3(\omega t) = \frac{1}{4}(3cos(\omega t) - cos(3\omega t))$$

$$sin^2(\omega t)cos(\omega t) = \frac{1}{4}(cos(\omega t) - cos(3\omega t))$$

In the calculation, we neglect term $\cos(3\omega t)$. So $cos^3(\omega t)$ and $sin^2(\omega t)cos(\omega t)$ can be presented as:

$$cos^3(\omega t) = \frac{3}{4}\cos(\omega t)$$

$$sin^2(\omega t)cos(\omega t) = 0.5cos(\omega t)$$

So, the previous expression is derived as

$$(b_3 A + \frac{3}{4}b_4 A^3 - A\omega^2 - A\omega^2 - 0.5b_1 A^3 \omega^4)\cos(\omega t) - (b_2 A\omega)\sin(\omega t) = psin(\omega t) +$$

$$Ecos(\omega t) \quad (4\text{-}13)$$

The same harmonic terms' coefficients are equating in equation (4-13) and using $F = \sqrt{p^2 + E^2}$ gives

$$((0.75b_4 - 0.5b_1\omega^4)A^3 + (b_3 - \omega^2)A)^2 + (b_2\omega A)^2 = F^2 \quad (4\text{-}14)$$

4.3 System Modeling and Analysis

The current-inductance response of linear inductor and nonlinear inductor are plotted shown, as shown in figure 4.1. The blue line is the I-L curve of the linear inductor. The inductance of the linear inductor does not vary with the current. The red curve represents the nonlinear I-L response. It can be seen that the NL inductor show very good nonlinear characteristics. The maximum inductance is around zero current points. As the current changes, the inductance behaves differently. The red curve is slightly higher than the blue curve at the maximum point. This is mainly because in the polynomial expression of nonlinear inductor, higher order terms are considered when

calculating. Because the coefficients L_n is involved in the I-L response of the NL inductor from the equation 4-2, resulting in that the coefficients are not optimized in figure 4.2, and one part line for the red curve is higher than the blue line. Through adjusting the coefficient, we can have a more perfect bell-shape curve in figure 4.2. The maximum inductance of the nonlinear inductor is the same as the linear inductor when the current is equal to zero.
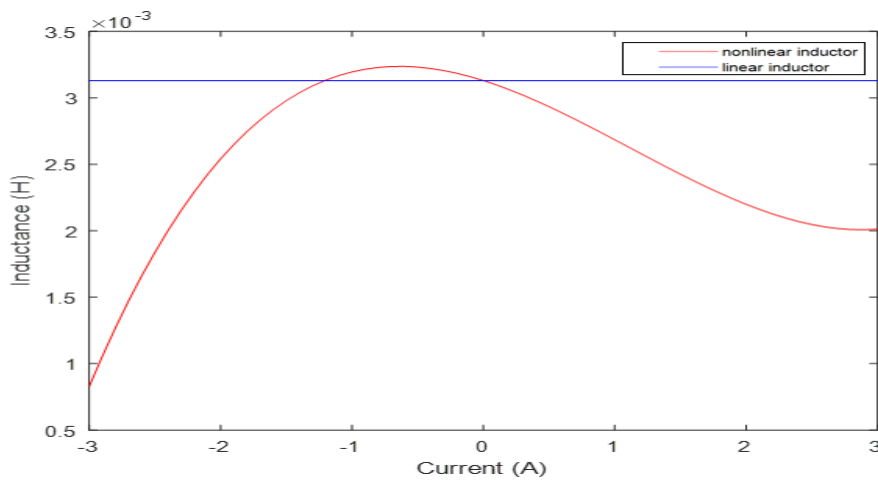
Figure 4.2 Current-Inductance responses of linear and nonlinear inductors
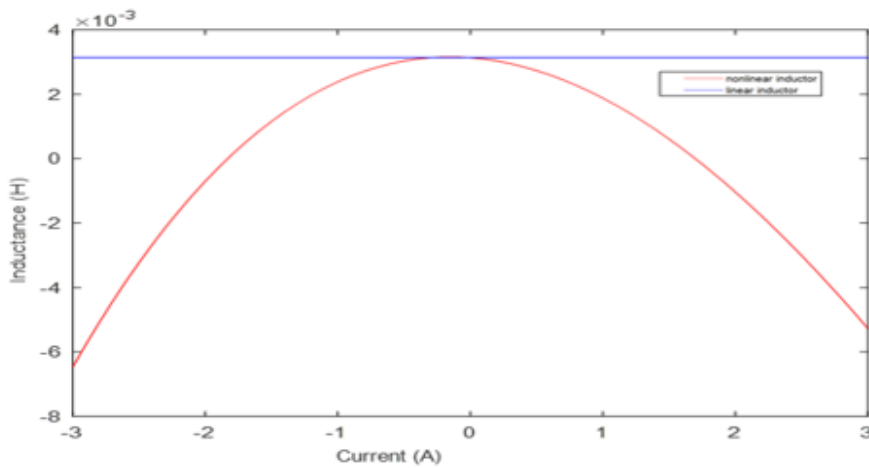
Figure 4.3 Optimal I-L curves of nonlinear inductor and linear inductor

Figures 4.4 and 4.5 show the amplitude-frequency relationship of the inductance at the different nonlinear coefficient of the nonlinear inductor.
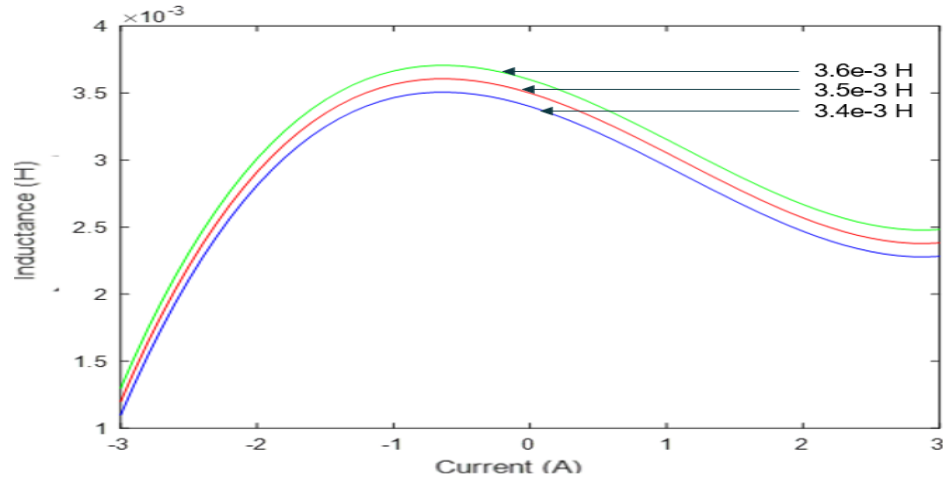
Figure 4.4 I-L curves of nonlinear inductor with different L0 values

L0 is the most important parameter in the nonlinear inductor, which determines the largest inductance when the current is at zero. Figure 4.4 presents the different I-L responses when the L0 value is changed. From fig.4.4, it is shown that as the L0 increases, the shape of the lines is almost same, but the slope of line and the maximum of the induction moves up.
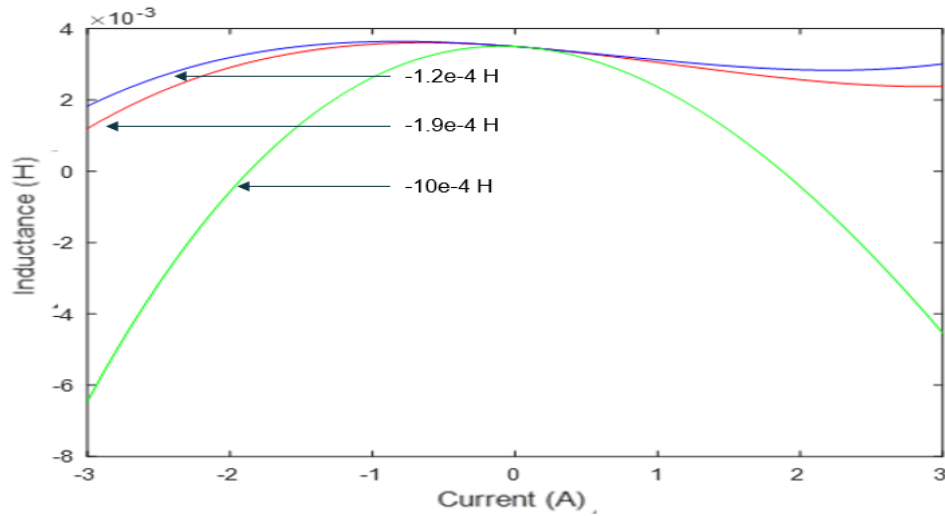
Figure 4.5 I-L curves of nonlinear inductor with different L2 values

The nonlinear characteristic of the nonlinear inductor depends on coefficient L2. As the value of L2 is getting smaller, the I-L curve becomes more curved. In figure 4.5, the red, blue, and green lines are cross when the current is zero. Except for this point, the blue line is higher than the others, which means that as the L2 value increases, the induction becomes larger when the circuit is the same. That is to say, only when the L2 is within the range from -10e to -4 H, the optimizing property of the nonlinear inductor can be obtained. In addition, it is also seen in figure 4.5, the maximum of the induction for the red and blue line are obtained when at current is a specific value. When the current is equal to zero, the inductance values are in maximum point.

By applying optimal parameters of nonlinear inductor into equation (4-14), we can have either amplitude-frequency response or amplitude-voltage response which are shown in figure 4.6 and figure 4.7. The blue curve is high equilibrium brunch, and the red curve is lower equilibrium brunch in the schematics. In figure 4.6, the three roots region is plotted as a blue curve. Moreover, the frequency response is till to the right which is

51

the high-frequency side. This region is also called the bistable interval. There are

coexisting solutions excited in this region. Only the blue curve and red curve are stable.

These two points are equilibrium points. The steady-state solution of the NCNL system

converges to the upper point or lower point is decided by the initial condition. When we

design the whole system the highest amplitude frequency point is the system frequency

because it can deliver maximum power to the load. Figure 4.7 shows the amplitude and

excitation voltage relationship at the desired. When the excitation voltage of the NCNL

system increases from 0 V, the response amplitude moves to the red curve. When the

voltage arrived around 40 V, the amplitude jumps up to the upper equilibrium blue

brunch. As the excitation voltage decreases, the amplitude response keeps at high

equilibrium brunch until the voltage decreases to nearly 0 V, and the jump down

phenomenon happens.
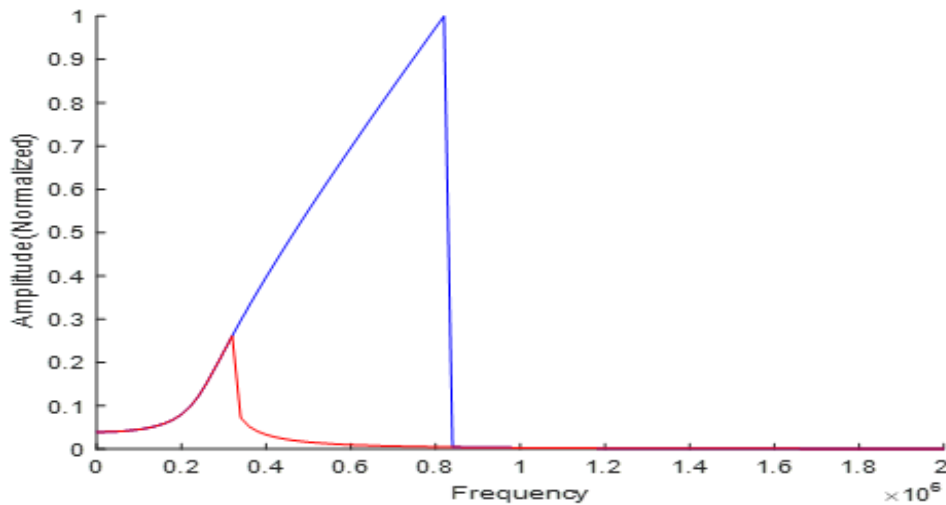
Figure 4.6 The amplitude-frequency response of NLNC system
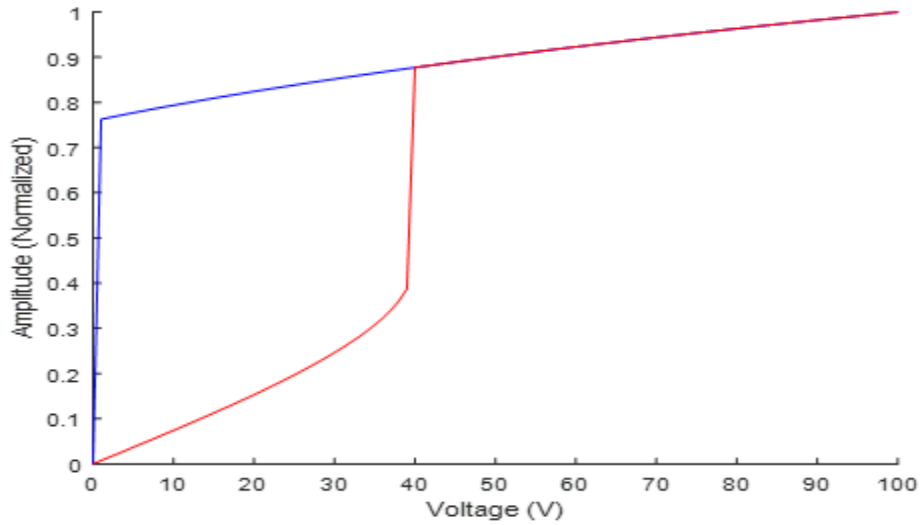
Figure 4.7 Amplitude-Voltage response of NCNL resonator. Blue curve is upper equilibrium brunch. Red curve is lower equilibrium brunch.

The different L0 of the nonlinear inductor coefficient can influence the jump down frequency point and bandwidth. In figure 4.8, the L0 values change from 2e-3 to 3.5e-3 H, respectively. As the value of L0 increased, the jump down frequency point is shifting to the right and the bandwidth is increased a little bit. The red curve peak and the blue curve peak slightly move to the right at the same time. However, the amplitude of the curves is almost the same.
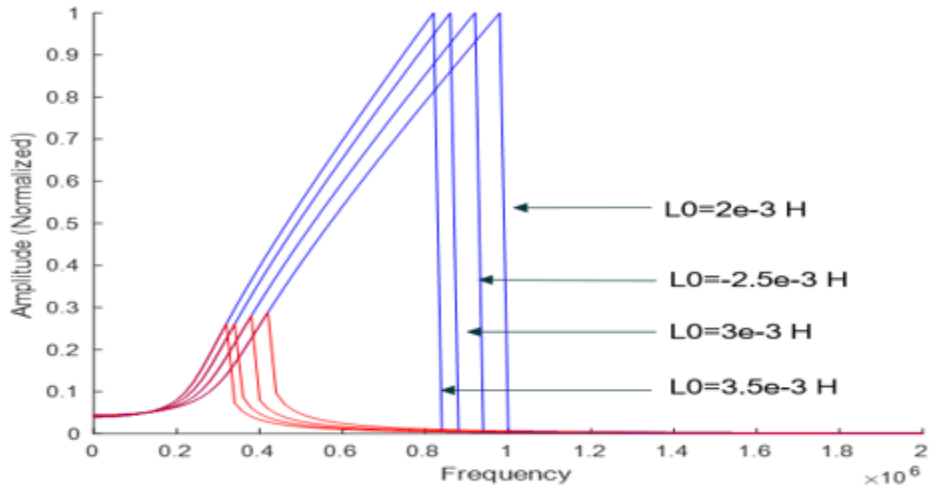
Figure 4.8 The amplitude-frequency responses of NLNC system with different L0 values

Figure 4.9 shows the NCNL circuit relationship of amplitude-frequency responses at different L2 from -10e-4 H to -1.9e-4 H. We observe that in the lower frequency region, the frequency-amplitude response curves corresponding to different L2 value are coincident, showing that the system exhibits almost the same nonlinear characteristics, bandwidth, and maximum amplitude. It means that nonlinear behavior and maximum amplitude of the system do not rely on L2 much. During the higher frequency region, when L2 increases, frequency-amplitude response curves move to the right side, showing stronger hardening behavior and increased bandwidth. However, the maximum amplitude remains unchanged. It means that the maximum amplitude of the system does not rely on L2. But the bandwidth can be influenced by L2 changing.
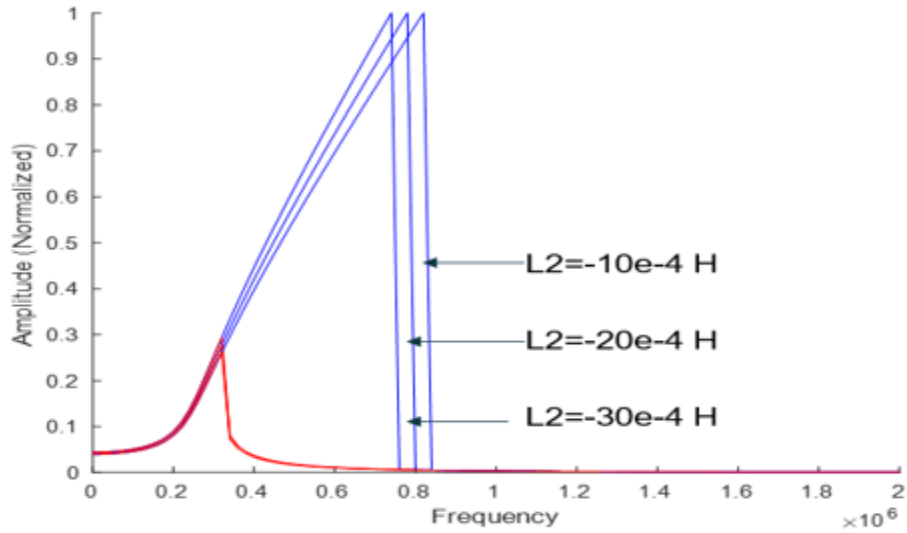
Figure 4.9 The amplitude-frequency responses of NLNC system with different L2 values
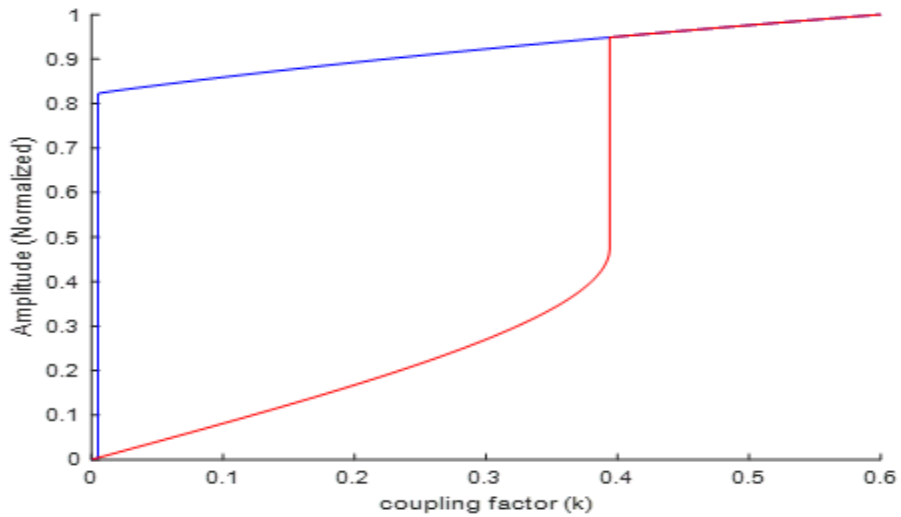
Figure 4.10 Amplitude-Frequency response of nonlinear inductor and nonlinear capacitor, NLNC, system with coupling factor changing

In the NCNL circuit, the equivalent Thevenin voltage of the wireless power transfer circuit is the function of the coupling factor. In reality, when the receiver resonator and transmitter get closer, the coupling factor is larger. So, the amplitude of the

equivalent voltage changes as the two resonators distance changing. The relationship of equivalent voltage and coupling factor is shown below.

$$U_e = \frac{V_s \omega M}{R_S} \tag{4-15}$$

Where U_e is equivalent Thevenin voltage. M is the mutual inductance and is a function of K. R_S is the inner resistance of source. And ω is angular frequency of excitation voltage. In the design, source voltage and excitation frequency are fixed. The only various parameter is mutual inductance, which is the coupling factor. So, when the mutual inductance or coupling factor increases, the amplitude of the equivalent voltage is increased. The relationship of coupling factor and amplitude for NCNL resonator is presented in figure 4.10. The blue curve is a high equilibrium point and red curve is the lower equilibrium point. The response of amplitude as a function of the coupling factor, K, is depicted in Fig. 10. When K increases from K = 0, the resonance amplitude increases slightly and moves on the lower equilibrium branch. When K reaches 0.4, a jump up in response to the upper equilibrium branch occurs. If K is decreased, a jump down occurs when K is close to the zero, representing the same trend as Amplitude-Voltage response shown as Fig4.7. Nonlinear resonant circuits are capable of adjusting their resonance frequencies based on the voltage amplitude across the nonlinear capacitors. Since the voltage amplitudes across the nonlinear capacitors in coupled nonlinear resonant circuits depend on the coupling factor, the resonance frequencies of the nonlinear resonators will be adjusted automatically based on the coupling factor. This self-adjustment characteristic is exploited to design the position insensitive WPT circuit.

4.4 NC and NCNL system comparison
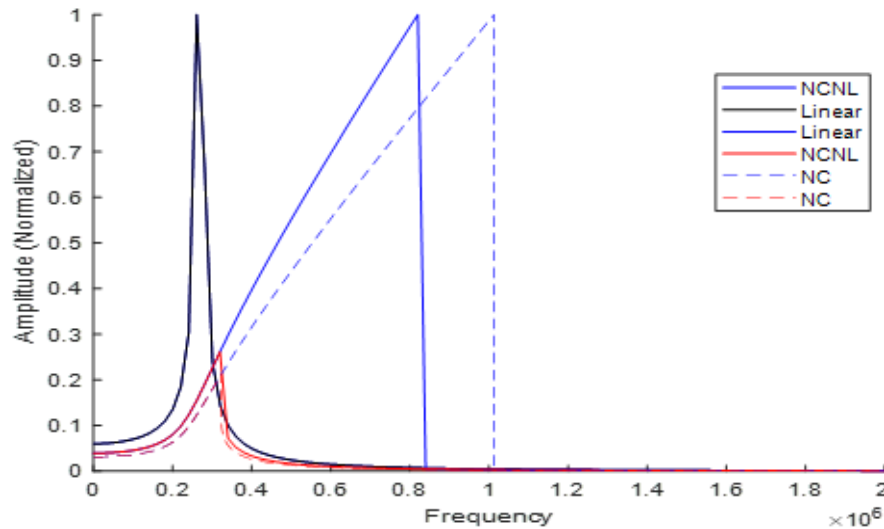
Figure 4.11 The amplitude-frequency response of the NCNL resonator circuit, in comparison with a LC circuit and duffing resonator with the same Q

Comparing to the amplitude-frequency response of NC duffing resonator, the

NCNL system has narrow bandwidth at the same quality factor. Although the bandwidth

is smaller than the NC system, it is still larger than the linear WPT system. The

amplitude-frequency responses of the three different systems is drawn in figure 4.11. All

the blue curves are high equilibrium brunch and red curves are lower equilibrium points.

The black curve in the figure is linear system response. Comparing with the linear RLC

circuit, the two branches of frequency-amplitude response curves for NC and NLNC

circuits bent to the left, showing the hardening behavior and resulting in increased

bandwidth. The maximum amplitude of the response stays unchanged. Moreover,

comparing the NC and NLNC circuits, although the bandwidth of the NLNC circuit is

slightly narrower than that of the NC circuit, the frequency value corresponding to the

maximum amplitude is respectively 0.8 MHz and 1.0 MHz for NLNC circuit and NC

circuit. It means that for the NLNC circuit, the same maximum amplitude as the NC

circuit can be obtained by using lower frequency value. Besides, during the lower

frequency region, the higher maximum amplitude value can be obtained by using the

NLNC circuit. It also means that better amplitude or efficiency can be achieved using the

NLNC circuit than by NC circuit when we design a WPT system with a lower frequency
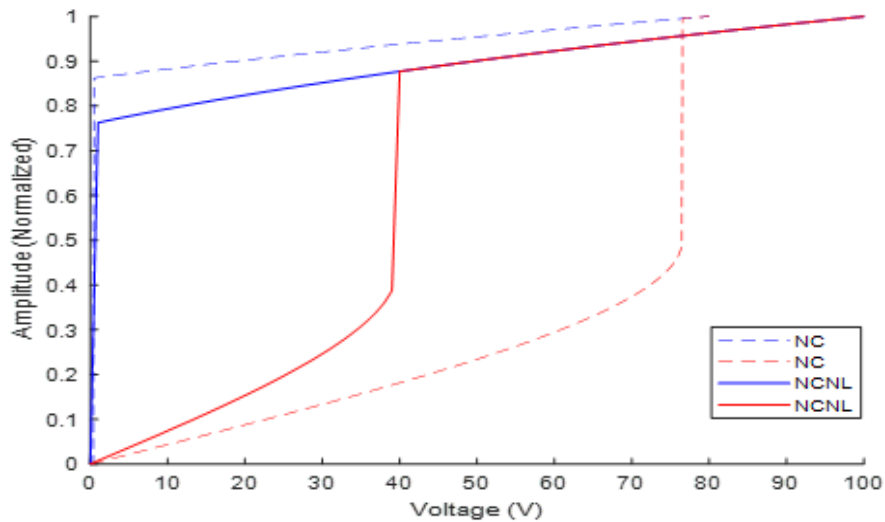
and higher quality factor.

Figure 4.12 The amplitude-voltage responses of NLNC resonator and NC duffing
resonator with the same quality factor.

In figure 4.12, the amplitude-voltage responses of NLNC resonator and NC

resonator are described. The blue curves are high equilibrium points and red curves are

lower equilibrium points. Under the same Q, the upper brunch of the NCNL circuit is

lower than this due to the nonlinear term L2 of nonlinear inductor. Comparing to the

jump up point of these two systems, the NCNL resonator needs less voltage to achieve

this phenomenon. The NC system needs almost double voltage if it wants to realize the

jump up phenomenon. In figure 4.13, When the two systems work at the same frequency,

the shapes of amplitude-voltage responses of NLNC and NC resonators are almost the same. The nonlinear capacitor system's amplitude dropping to the NCNL point is due to the excitation voltage of NC tuning down to the NCNL maximum frequency point. The NC quality factor is less than NCNL.
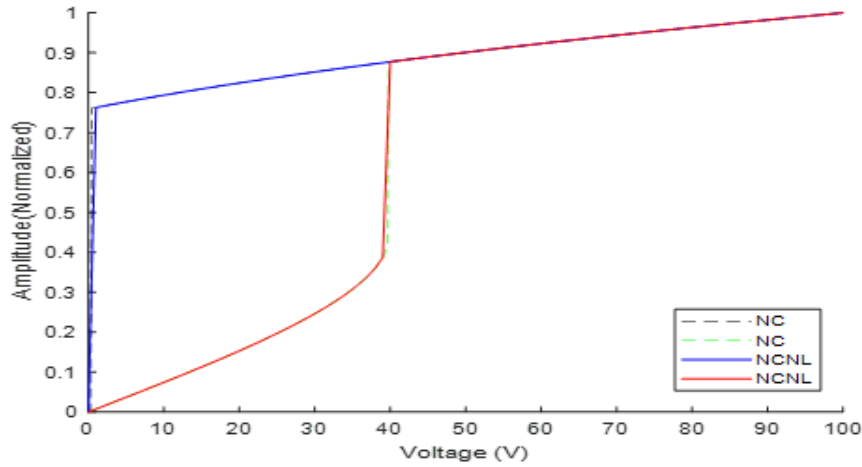
Figure 4.13 The amplitude-voltage responses of NLNC resonator and NC duffing resonator at the same excitation frequency.
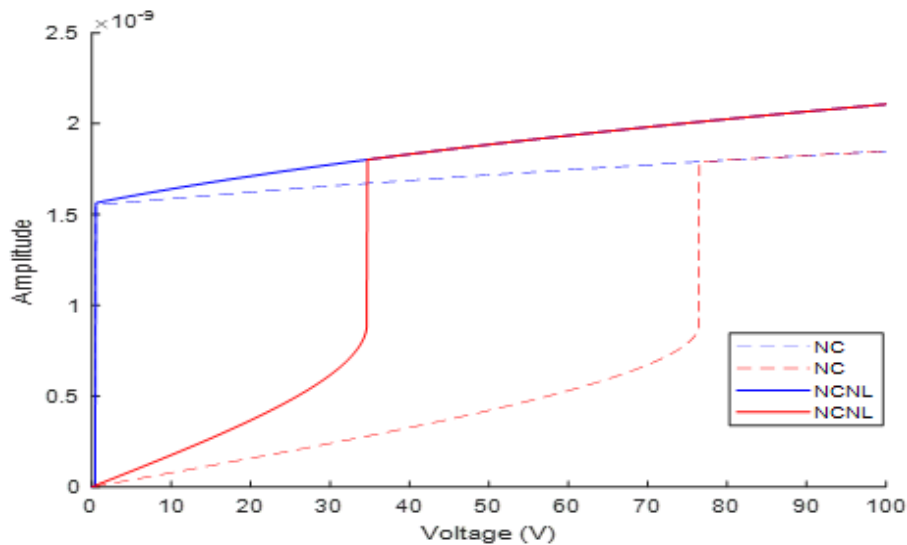
Figure 4.14 The amplitude-voltage response of NLNC resonator and NC duffing resonator starting at the same amplitude.

Figure 4.14 shows the amplitude frequencies of the NLNC system and NC system start at the same amplitude. The blue curves and red curves represent the high equilibrium brunch and lower equilibrium brunch, respectively. Comparing to the nonlinear capacitor duffing resonator, a nonlinear capacitor with a nonlinear inductor resonator has a better amplitude than NC resonator. Moreover, the needed jump up the voltage of the NLNC circuit is also smaller than the NC circuit. It means when the system unfortunate excites at lower frequency brunch. The NLNC system needs less power to jump up to the high equilibrium brunch while the NC resonator needs twice the time voltage than the NLNC system. Moreover, the peak amplitude of NLNC is larger than NC, representing more power that could be delivered to the load, and the efficiency is better than the NC resonator under the same amplitude voltage source.

In the wireless power transfer system design, the mutual inductance is the function of distance. So, at the same time, the coupling factor is also as the function of distance. The expressions are presented in [78]:

$$M = \frac{\mu \pi n_1 n_2 a^2 b^2}{\sqrt{(a+b)^2 + d^2}[(a-b)^2 + d^2]} \tag{4-16}$$

Where μ is permeability of free space. n_1 and n_2 are the two coils terms. a and b are the radius of the coils. d is the distance between the two coils. In order to simplify the calculation. We assume that all the parameters of two coils are the same, $n_1 = n_2 = 10$, and a=b=10 mm. Due to the coupling factor is k=M/$\sqrt{L_1 L_2}$. So, the response of distance and coupling factor is shown in figure 4.15. As the two coils distance increasing from 0, the coupling factor decreases from 0.56 to 0. It indicates that when the two coils air gap

becomes larger, the coupling capability of the tow coils is getting weak. As the distance become larger, the coupled energy is reducing.
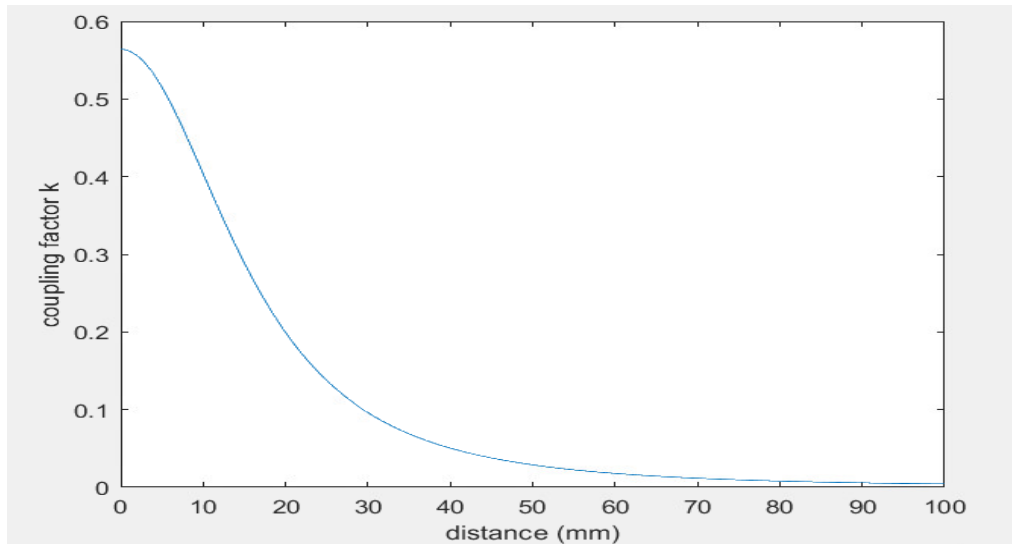
Figure 4.15 Coupling factor as a function of distance

The relationship between amplitude and two coils' distance response is presented in figure 4.16. The proposed NCNL system could maintain a high amplitude when the distance of the system is different. It also indicates the system efficiency can keep at high value when the distance is changing. The NCNL system effectively solves the problem of frequency splitting. When the distance between the two resonator coils increasing from zero to 100 mm, as shown in figure 4.16, the system's amplitude decreases a little bit but still situates above 0.7. This system could be applied to various charging applications without considering the power transfer efficiency reduced by distance changing of transmitter and receiver.
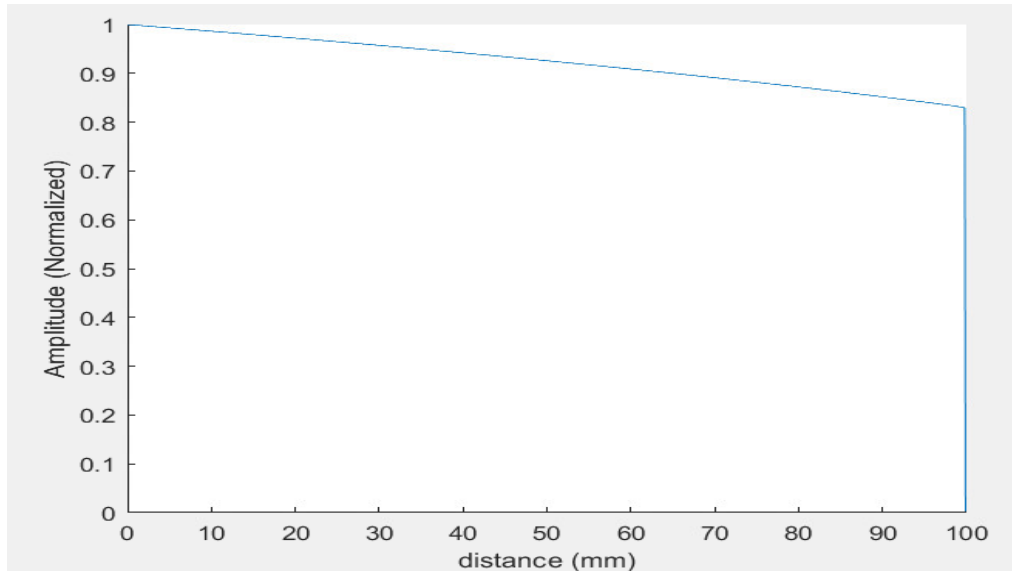
Figure 4.16 Amplitude-distance response of NLNC system

In order to furtherly improve properties of WPT, this chapter design a higher efficient nonlinear resonator with nonlinear ferromagnetic thin film core inductors and nonlinear ferroelectric thin film dielectrics capacitors and derives a new of nonlinear differential equations governing the nonlinear dynamical behavior of the nonlinear resonator. The obtained numerical results display that the new system presents good softening behavior. The effects of different parameters on the system behavior are discussed. It is found that the parameters of the nonlinear components can be used to control the amplitude of the nonlinear response of the NCNL system. Finally, the properties between the new system and the duffing resonator and linear RLC circuit are compared. The results show that compared with the linear RLC circuit, the NCNL resonator and duffing resonator show the hardening behavior and result in increased bandwidth. Although the bandwidth of the new NCNL system is slightly narrower than that of NC circuit, in the lower frequency region, the higher maximum amplitude value can be obtained by using this system, which means that better efficiency can be achieved

by using the new system when we design a WPT system with a lower frequency and higher quality factor. Besides, by comparison between amplitude- voltage response curves of NC circuit and new system, we can be found that circuit, to maintain high PTE values, the much lower excitation voltage value is required for the new system. As an up- and-coming solution, the new system will have broad application prospects in many wireless power transfer fields without adding active circuits to track the frequency.

CHAPTER 5

CONCLUSION

5.1 Summary

This thesis overviews the research status and trend of WPT technologies, analyses the frequency splitting phenomenon for wireless power transfer system, discusses the duffing resonator circuit and its properties, and design a kind of high-efficiency wireless power transfer inductive system with both non-linear inductors and non-linear capacitors. The main research conclusion of this paper is as follows:

Firstly, the research status and trend of WPT technologies are overviewed. The characteristics, principles of operation, research status, and critical problems of the four mainstream WPT technologies are elaborated, analyzed, and compared. Application researches of the technology in wireless charging, bio-implants transportation, and consumer electronics fields are summarized.

Secondly, aiming at the frequency splitting problem during magnetic coupled resonance wireless power transmission, a system model was built based on the theory of mutual inductance coupling, the power, and efficiency expressions of conventional two coils CPT system is presented. Meanwhile, by analyzing the response of PTE versus resonant frequency versus coupling factor, the frequency characteristics, regularity, and occurrence condition of the frequency splitting phenomenon for the magnetic resonant

coupling WPT system are summarized. Moreover, the frequency splitting phenomena are analyzed with the power transfer capability S21 and the system efficiency curves at different coupling by the aid of simulation. The results show that the three regions are existing in the WPT system. They are over-coupled range, critically coupled range, and under-coupled range. The frequency splitting phenomena only occur in the over-coupled region. The S21 and efficiency split into two peak values. Finally, the frequency splitting suppression methods are proposed. The above research work provides a theoretical basis for solving the problem of frequency splitting and designing a kind of high-efficiency WPT system.

Thirdly, a duffing resonator circuit with nonlinear capacitor, which can eliminate the frequency splitting and keep the high transmission efficiency and power delivered to the load is developed. With the help MATLAB software, the properties of the duffing resonance circuit are discussed. The results show duffing resonator can not only exhibit a significant advantage in improving the WPT system's tolerance to coupling factor variations without degrading the system's efficiency but also having more wider bandwidth with a conventional linear resonator. Therefore, it is an up-and-coming solution in designing WPT systems that require insensitivity to coupling factor variations.

Finally, to further improve properties of WPT, we design a higher efficient nonlinear resonator with nonlinear ferromagnetic thin film core inductors and nonlinear ferroelectric thin film dielectrics capacitors and derives the nonlinear differential equations governing the nonlinear dynamical behavior of the nonlinear resonator. The obtained numerical results show that the new system presents good hardening behavior. The effects of different parameters on the system behavior are discussed.

5.2 Future work

NCNL circuit has been successfully simulated in MATLAB. In future works, we will apply this circuit into the experiment and real applications to test the performance and properties for the response of efficiency and distance. In the next step's experiment, except test the needed phenomenon, we will also try to use different material made nonlinear inductors and nonlinear capacitors in the test. By using different types components, we want to achieve best performance of the power transfer efficiency response. Multi receiver resonators also be an important study in future design. Because in reality, one source to multiple devices charging is needed, such as the multiple phone charging in the same room. So, this study could provide an efficient method to solve the space occupation when charging many devices.

REFERENCES

[1]   J. Dai and D. Ludois, "A survey of wireless power transfer and a critical comparison of inductive and capacitive coupling for small gap applications," IEEE Trans. Power Electron., vol. 30, no. 11, pp. 6017–6029, Nov. 2015.

[2]   F. Lu, H. Zhang, H. Hofmann, and C. Mi, "A double-sided LCLC compensated capacitive power transfer system for electric vehicle charging," IEEE Trans. Power Electron., vol. 30, no. 11, pp. 6011–6014, Nov. 2015.

[3]   H. Zhang, F. Lu, H. Hofmann, W. Liu, and C. Mi, "A four-plate compact capacitive coupler design and LCL-compensated topology for capacitive power transfer in electric vehicle charging application," IEEE Trans. Power Electron., vol. 31, no. 12, pp. 8541–8551, Dec. 2016

[4]   Jadidian, Jouya, and Dina Katabi. "Magnetic MIMO: How to Charge Your Phone in Your Pocket." Proceedings of the 20th Annual International Conference on Mobile Computing and Networking, 2014, pp. 495–506.

[5]   P. S. Riehl et al., "Wireless power systems for mobile devices supporting inductive and resonant operating modes," IEEE Trans. Microw. Theory Techn., vol. 63, no. 3, pp. 780–790, Mar. 2015.

[6]   M. Mohammad, S. Choi, Z. Islam, S. Kwak and J. Baek, "Core Design and Optimization for Better Misalignment Tolerance and Higher Range of Wireless Charging of PHEV," in IEEE Transactions on Transportation Electrification, vol. 3, no. 2, pp. 445-453, June 2017.

[7]   Vilathgamuwa, D. Mahinda and J. P. K. Sampath. "Chapter 2 Wireless Power Transfer (WPT) for Electric Vehicles (EVs) — Present and Future Trends." 2017.

[8]   J. S. Ho, S. Kim and A. S. Y. Poon, "Midfield wireless powering for implantable systems", Proc. IEEE, vol. 101, no. 6, pp. 1369–1378, Jun. 2013.

[9]   P. Si, A. P. Hu, J. W. Hsu, M. Chiang, Y. Wang, S. Malpas, and D. Budgett, "Wireless power supply for implantable biomedical device based on primary input voltage regulation," in Proc. 2nd IEEE Conf. Ind. Electron. Appl., 2007, pp. 235–239.

[10]   P. Si, A. P. Hu, S. Malpas, and D. Budgett, "A frequency control method for regulating wireless power to implantable devices," IEEE Trans. Biomed. Circuits Syst., vol. 2, no. 1, pp. 22–29, Mar. 2008.

[11]   http://industryarc.com/Report/7384/wireless-charging-market-report.html.

[12]   Brown, W.C. The history of power transmission by radio waves. IEEE Trans. Microw. Theory Tech. 1984, 32, 1230–1242.

[13]   Brown W C. The history of wireless power transmission[J]. Solar Energy, 1996, 56(1): 3-23.

[14]   Glaser P E. Power from the Sun: Tis Future[J]. Science, 1968, 162(3856): 857-861.

[15]   Matsumoto H. Research on solar power satellites and microwave power transmission in Japan[J]. IEEE Microwave Magazine, 2002, 3(4): 36-45.

[16]   Nansen R H. Wireless power transmission：the key to solar power satellites[J]. IEEE Transactions on Aerospace and Electronic Systems Magazine, 1996, 11(1): 33-39.

[17]   Green A, Boys J. Inductively coupled power transmission-concept, design, and
application[J]. Transactions of the Institution of Professional Engineers New
Zealand Electrical/mechanical/ chemical Engineering, 1995, 22(1): 1-9.

[18]   Kurs A, Karalis A, Moffatt R, et al. Wireless power transfer via strongly coupled
magnetic resonances[J]. Science, 2007, 317(5834): 83-86.

[19]   Yang Xuexia. Overview of microwave power transmission technology and recent
progress of rectennas [J]. Chinese Journal of Radio Science, 2009, 24(4): 770-
779.

[20]   He Tao, Yang Suhui, Zhang Haiyang, et al. Experiment of space laser energy
transmission and conversion with high efficiency[J]. Chinese Journal of Lasers,
2013, 40(3): 1-6.

[21]   N. Tesla, "Apparatus for transmitting electrical energy," U.S. Patent 1119732,
Dec. 1, 1914.

[22]   Fu W Z, Zhang B, Qiu D Y, et al. Maximum efficiency analysis and design of
self-resonance coupling coils for wireless power transmission system. Proc
CSEE,2009, 29(18): 21–26 .

[23]   Sedwick R J. Long rang inductive power transfer with superconducting
oscillators. Ann Phys, 2010, 25:287–299.

[24]   Mizuno, T.; Yachi, S.; Kamiya, A.; Yamamoto, D. Improvement in efficiency of
wireless power transfer of magnetic resonant coupling using magnetoplated wire.
IEEE Trans. Magn. 2011, 47, 4445–4448.

[25]   Wang C S, Covic G A, Stielau O H. Power transfer capability and bifurcation phenomena of loosely coupled inductive power transfer systems. IEEE Trans Indus Electron, 2004, 51: 148–157.

[26]   S. Assawaworrarit, X. Yu, and S. Fan, "Robust wireless power transfer using a nonlinear parity–time-symmetric circuit," Nature, vol. 546, pp. 387–390, Jun. 2017.

[27]   X. Y. Zhang, C.-D. Xue, and J.-K. Lin, "Distance-insensitive wireless power transfer using mixed electric and magnetic coupling for frequency splitting suppression," IEEE Trans. Microw. Theory Techn., vol. 65, no. 11, pp. 4307–4316, Nov. 2017.

[28]   Chang, C.-W.; Hou, K.-C.; Shieh, L.-J.; Hung, S.-H.; Chiou, J.-C. Wireless powering electronics and spiral coils for implant microsystem toward nanomedicine diagnosis and therapy in free-behavior animal. Solid-State Electron. 2012, 77, 93–100.

[29]   Li, X.H.; Zhang, H.R.; Peng, F.; Li, Y.; Yang, T.Y.; Wang, B.; Fang, D.M. A wireless magnetic resonance energy transfer system for micro implantable medical sensors. Sensors 2012, 12, 10292–10308.

[30]   http://www.google.com.hk/imglanding.

[31]   http://www.52solution.com/article/articleinfo/id/80010144/page/3.

[32]   Kim, J.; Son, H.-C.; Kim, D.-H.; Park, Y.-J. Optimal design of a wireless power transfer system with multiple self-resonators for an led tv. IEEE Trans. Consum. Electron. 2012, 58, 775–780.

[33]   Sallan, J.; Villa, J.L.; Llombart, A.; Sanz, J.F. Optimal design of icpt systems applied to electric vehicle battery charge. IEEE Trans. Ind. Electron. 2009, 56, 2140–2149.

[34]   Villa, J.L.; Sallán, J.; Llombart, A.; Sanz, J.F. Design of a high frequency inductively coupled power transfer system for electric vehicle battery charge. Appl. Energy 2009, 86, 355–363.

[35]   Imura, T.; Okabe, H.; Hori, Y. Basic Experimental Study on Helical Antennas of Wireless Power Transfer for Electric Vehicles by Using Magnetic Resonant Couplings. In Proceedings of the Vehicle Power and Propulsion Conference (VPPC '09), Dearborn, MI, USA, 7–10 September 2009; pp. 936–940.

[36]   Covic, G.A.; Boys, J.T. Modern trends in inductive power transfer for transportation applications. IEEE J. Emerg. Sel. Top. Power Electron. 2013, 1, 28–41.

[37]   Bolger, J.G.; Kirsten, F.A.; Ng, L.S. Inductive Power Coupling for an Electric Highway System. In Proceedings of the 28th IEEE Vehicular Technology Conference, Denver, CO, USA, 22–24 March 1978; pp. 137–144.

[38]   Xu, Q.; Wang, H.; Gao, Z.; Mao, Z.-H.; He, J.; Sun, M. A novel mat-based system for position-varying wireless power transfer to biomedical implants. IEEE Trans. Magn. 2013, 49, 4774–4779.

[39]   Xie, L.; Shi, Y.; Hou, Y.T.; Sherali, H.D. Making sensor networks immortal: An energy-renewal approach with wireless power transfer. IEEE/ACM Trans. Netw. 2012, 20, 1748–1761.

[40]   T. Campi, S. Cruciani, M. Feliziani and A. Hirata, "Wireless power transfer system applied to an active implantable medical device," 2014 IEEE Wireless Power Transfer Conference, Jeju, 2014, pp. 134-137.

[41]   K. S. Keerthi., K. Ilango. and G. N. Manjula., "Study of Midfield Wireless Power Transfer for Implantable Medical Devices," 2018 2nd International Conference on Biomedical Engineering (IBIOMED), Kuta, 2018, pp. 44-47.

[42]   Y. Zhao, X. Tang, Z. Wang and W. T. Ng, "An Inductive Power Transfer System With Adjustable Compensation Network For Implantable Medical Devices," 2019 IEEE Asia Pacific Conference on Circuits and Systems (APCCAS), Bangkok, Thailand, pp. 209-212, 2019.

[43]   S. Xu, H. Zhang, C. Yao, D. Ma, N. Jin and H. Tang, "Eigenvector Lookup Position Detection Method for Wireless Power Transfer of Electric Vehicles," 2019 IEEE PELS Workshop on Emerging Technologies: Wireless Power Transfer (WoW), London, United Kingdom, pp. 177-180, 2019.

[44]   A. Ramezani and M. Narimani, "A Wireless Power Transfer System with Reduced Output Voltage Sensitivity for EV Applications," 2018 IEEE PELS Workshop on Emerging Technologies: Wireless Power Transfer (Wow), Montréal, QC, 2018, pp. 1-5.

[45]   Y. Hsieh, Z. Lin, M. Chen, H. Hsieh, Y. Liu and H. Chiu, "High-Efficiency Wireless Power Transfer System for Electric Vehicle Applications," in IEEE Transactions on Circuits and Systems II: Express Briefs, vol. 64, no. 8, pp. 942-946, Aug. 2017, doi: 10.1109/TCSII.2016.2624272. Jianyu, L., Houjun, T., & Xin, G. (2013).

[46] A. P. Sample, D. A. Meyer, J. R. Smith, "Analysis, experimental results, and range adaptation of magnetically coupled resonators for wireless power transfer", IEEE Trans. on Industrial Electronics, vol.58, pp544-554, 2001.

[47] M. W. Baker, R. Sarpeshkar, "Feedback analysis and design of rf power links for low-power bionic systems", IEEE Trans. on Biomedical Circuits and Systems, vol. 1, pp. 28–38, 2007. [Online].

[48] N. Wang-Qiang, C. Jian-Xin, G. Wei, S. Ai-Di, "Exact analysis of frequency splitting phenomena of contactless power transfer systems", IEEE Trans. on Circuits and Systems I: Regular Papers, vol. 60, pp.1670–1677, 2013.

[49] W. Q. Niu, W. Gu, J. X. Chu, A. D. Shen, "Coupled-mode analysis of frequency splitting phenomena in CPT systems", Electronics Letters, vol. 48, pp. 723–724, 2012.

[50] Agbinya, J.I., Nguyen, H. Principles and Applications of Frequency Splitting in Inductive Communications and Wireless Power Transfer Systems. Wireless Pers Commun 107, pp. 987–1017, 2019.

[51] Liu, J.; Wang, C.; Wang, X.; Ge, W. Frequency Splitting and Transmission Characteristics of MCR-WPT System Considering Non-Linearities of Compensation Capacitors. Electronics 2020, 9, 141.

[52] Niu, Wangqiang, Wei Gu, and Jianxin Chu. "Analysis and experimental results of frequency splitting of underwater wireless power transfer." The Journal of Engineering, pp. 385-390, 2017.

[53] Kurs, A.; Moffatt, R.; Soljacic, M. Simultaneous mid-range power transfer to multiple devices. Appl. Phys. Lett. 2010, 96, doi:10.1063/1.3284651.

[54] Fei, Z.; Hackworth, S.A.; Weinong, F.; Chengliu, L.; Zhihong, M.; Mingui, S. Relay effect of wireless power transfer using strongly coupled magnetic resonances. IEEE Trans. Magn. 2011, 47, 1478–1481.

[55] Kim, J.W.; Son, H.-C.; Kim, K.-H.; Park, Y.-J. Efficiency analysis of magnetic resonance wireless power transfer with intermediate resonant coil. IEEE Antennas Wirel. Propag. Lett. 2011, 10, 389–392.

[56] Kim, J.-W.; Son, H.-C.; Kim, D.-H.; Kim, K.-H.; Park, Y.-J. Analysis of Wireless Energy Transfer to Multiple Devices using CMT. In Proceedings of the Asia-Pacific Microwave Conference Proceedings (APMC), Yokohama, Japan, 7–10 December 2010; pp. 2149–2152.

[57] Soljačić M, Kurs A, Karalis A, et al. Wireless power transfer via strongly coupled magnetic resonances. Sci Express, 2007, 317(5834): 83–86.

[58] Haus H A. Waves and Fields in Optoelectronics. New Jersey: Prentice-Hall Ltd, 1984.

[59] N.Tesla, "System of Transmission of Electrical Energy," U.S. Patent 645,576, 20 Mar 1900.

[60] J. Lee, Y.-S. Lim, W.-J. Yang, and S.-O. Lim, "Wireless power transfer system adaptive to change in coil separation," IEEE Trans. Antennas Propag., vol. 62, no. 2, pp. 889–897, Feb. 2014.

[61] O. Abdelatty, X. Wang and A. Mortazawi, "Position-Insensitive Wireless Power Transfer Based on Nonlinear Resonant Circuits," in IEEE Transactions on Microwave Theory and Techniques, vol. 67, no. 9, pp. 3844-3855, Sept. 2019.

[62]   X. Zan and A. Avestruz, "Wireless power transfer for implantable medical devices using piecewise resonance to achieve high peak-to-average power ratio," 2017 IEEE 18th Workshop on Control and Modeling for Power Electronics (COMPEL), Stanford, CA, 2017, pp. 1-8.

[63]   S. Huang, Z. Li and K. Lu, "Frequency splitting suppression method for four-coil wireless power transfer system," in IET Power Electronics, vol. 9, no. 15, pp. 2859-2864, 14 12 2016.

[64]   Jordan, Dominic William, and Peter Smith. Nonlinear Ordinary Differential Equations: Problems and Solutions. Oxford: Oxford University Press, 2007.

[65]   Dai, Xin, et al. "A Maximum Power Transfer Tracking Method for WPT Systems with Coupling Coefficient Identification Considering Two-Value Problem." Energies, vol. 10, no. 10, 2017, p. 1665.

[66]   M. W. Baker, R. Sarpeshkar, "Feedback analysis and design of rf power links for low-power bionic systems", IEEE Trans. on Biomedical Circuits and Systems, vol. 1, pp. 28–38, 2007. [Online].
Available:http://dx.doi.org/10.1109/TBCAS.2007.893180

[67]   T. C. Beh, M. Kato, T. Imura, S. Oh, and Y. Hori, "Automated impedance matching system for robust wireless power transfer via magnetic resonance coupling," IEEE Trans. Ind. Electron., vol. 60, no. 9, pp. 3689–3698, Sep. 2013.

[68]   W. Zhong and S. Y. R. Hui, "Charging Time Control of Wireless Power Transfer Systems Without Using Mutual Coupling Information and Wireless Communication System," in IEEE Transactions on Industrial Electronics, vol. 64, no. 1, pp. 228-235, Jan. 2017.

[69]   Mai, R.; Liu, Y.; Li, Y.; Yue, P.; Cao, G.; He, Z. An Active Rectifier Based

          Maximum Efficiency Tracking Method Using an Additional Measurement Coil

          for Wireless Power Transfer. IEEE Trans. Power Electron. 2018, 33, 716–728.

[70]   Lullo, Giuseppe et al. "Non-linear inductor modelling for a DC/DC Buck

          converter." Renewable energy & power quality journal 1 (2017): 686-693.

[71]   Kpomahou, Y. J. F., et al. "Nonlinear Resonances Analysis of a RLC Series

          Circuit Modeled by a Modified Van der Pol Oscillator."

[72]   Wang, Xinning et al. "A Nonlinear Circuit Analysis Technique for Time-Variant

          Inductor Systems." Sensors (Basel, Switzerland) vol. 19,10 2321. 20 May. 2019,

          doi:10.3390/s19102321.

[73]   D. Scirè, S. Rosato, G. Lullo and G. Vitale, "A Temperature Dependent Non-

          Linear Inductor Model for a DC/DC Boost Converter," 2018 15th International

          Conference on Synthesis, Modeling, Analysis and Simulation Methods and

          Applications to Circuit Design (SMACD), Prague, 2018, pp. 237-9, doi:

          10.1109/SMACD.2018.8434880.

[74]   Kovacic, I., & Brennan, M. J. (2011). The Duffing equation: Nonlinear oscillators

          and their behavior. Wiley.com.

[75]   Chase DR, Chen LY, York RA. Modeling the capacitive nonlinearity in thin-film

          BST varactors. IEEE Transactions on Microwave Theory and Techniques, 2005

          Oct;53(10):3215-20.

[76]   Xiaoyu Wang. High Efficiency and High Sensitivity Wireless Power Transfer and

          Wireless Power Harvesting Systems. 2016.

[77]   Li, L.M. & Billings, S.A. (2009). Analysis of nonlinear oscillators in the

frequency domain using volterra series Part II : identifying and modelling jump

Phenomenon.

[78]   Duarte, Rafael Mendes, and Gordana Klaric Felic. "Analysis of the Coupling

Coefficient in Inductive Energy Transfer Systems." Active and Passive Electronic

Components, vol. 2014, 2014, pp. 1–6.